CHALMERS

Modeling and Simulation of Transient Fault Response at Lillgrund Wind Farm when Subjected to Faults in the Connecting 130 kV Grid

Master of Science Thesis in Electric Power Engineering

ANDERS ELIASSON
EMIR ISABEGOVIĆ

Modeling and Simulation of Transient Fault Response at Lillgrund Wind Farm when Subjected to Faults in the Connecting 130 kV Grid

Anders Eliasson   Emir Isabegović

Department of Energy and Environment
CHALMERS UNIVERSITY OF TECHNOLOGY
Göteborg, Sweden 2009

Modeling and Simulation of Transient Fault Response at Lillgrund Wind Farm when Subjected to Faults in the Connecting 130 kV Grid

Anders Eliasson
Emir Isabegović

Department of Energy and Environment
CHALMERS UNIVERSITY OF TECHNOLOGY
SE-412 96 Göteborg
Sweden
Telephone + 46 (0)31 772 16 44

Abstract

The purpose of this thesis was to investigate what type of faults in the connecting grid should be dimensioning for future wind farms. An investigation of over and under voltages at the main transformer and the turbines inside Lillgrund wind farm was the main goal. The results will be used in the planning stage of future wind farms when performing insulation coordination and determining the protection settings.

A model of the Lillgrund wind farm and a part of the connecting 130 kV grid were built in PSCAD/EMTDC. The farm consists of 48 Siemens SWT-2.3-93 2.3 MW wind turbines with full power converters. The turbines were modeled as controllable current sources providing a constant active power output up to the current limit of 1.4 pu. The transmission lines and cables were modeled as frequency dependent (phase) models.

The load flows and bus voltages were verified towards a PSS/E model and the transient response was verified towards measuring data from two faults, a line to line fault in the vicinity of Barsebäck (BBK) and a single line-to-ground fault close to Bunkeflo (BFO) substation. For the simulation, three phase to ground, single line to ground and line to line faults were applied at different locations in the connecting grid and the phase to ground voltages at different buses in the connecting grid and at turbines were studied. These faults were applied for different configurations of the farm.

For single line to ground faults, the highest over voltage on a turbine was 1.22 pu (32.87 kV) due to clearing of a fault at BFO (the PCC). For line to line faults, the highest over voltage on a turbine was 1.59 pu (42.83 kV) at the beginning of a fault at KGE one bus away from BFO. Both these cases were when all radials were connected and the turbines ran at full power. The highest over voltage observed at Lillgrund was 1.65 pu (44.45 kV). This over voltage was caused by a three phase to ground fault applied at KGE and occurred at the beginning of the fault and when all radials were connected and the turbines ran in idle operation. For all simulated configurations, the highest over voltage occurred at the turbine located at the end of the longest radial.

The highest over voltages on the main transformer were 1.56 pu (42.03 kV) on the low voltage side and caused by a three-phase fault at KGE and 1.17 pu (131.9 kV) on the high voltage side from a phase-to-phase fault at BFO.

The most severe voltage dip occurred on turbine E-02 with 0.014 pu (0.38 kV) remaining voltage and was caused by a three phase to ground fault at BFO. This occurred when only that radial was connected.

The amount of power generated and radials connected affected the maximum over and under voltage levels. Lower power generation resulted in higher over voltages and more severe voltage dips at the turbines. Fewer radials resulted in lower over voltages and less severe voltage dips.

Acknowledgement

Svensk sammanfattning

Detta examensarbete syftar till att utreda vilka typer av fel i det anslutande nätet som är dimensionerande för vindkraftparker. Huvudsyftet med arbetet var att undersöka över- och underspänningar på huvudtransformatorn och turbinerna i Lillgrunds vindkraftspark. Resultaten är tänkta att användas i planeringsstadiet för framtida vindkraftparker vid genomförande av isolationskoordinering samt bestämmande av skyddsinställningar.

Under projektets genomförande byggdes i PSCAD/EMTDC en modell av Lillgrunds vindkraftpark samt en del av det anslutande 130 kV-nätet. Parken består av 48 stycken Siemens SWT-2,3-93 2,3 MW vindturbiner med fulleffektsomriktare. Turbinerna modellerades som styrbara strömkällor som styrdes så att de gav konstant aktiv effekt upp till en maximal ström på 1,4 pu. Kraftledningar och kablar modellerades med frekvensberoende (fas) modeller.

Lastflöden och spänningar i modellen verifierades gentemot desamma från en PSS/E-modell och det transienta svaret verifierades mot mätdata från två olika fel, ett enfasfel i närheten av Bunkeflo station och ett tvåfasfel nära Barsebäck. Under simuleringarna applicerades enfas-, tvåfas- och trefasfel på olika ställen i nätet varefter spänningarna mellan fas-jord registrerades, både i det anslutande nätet och i parken. Dessa fel applicerades för olika konfigurationer av parken.

För enfasfel gäller att den högsta observerade överspänningen på någon turbin var 1,22 pu (32,87 kV) då ett fel på den anslutande bussen (PCC) i BFO kopplades bort. Högsta observerade överspänningen på någon turbin orsakad av ett tvåfasfel var 1,59 pu (42,83 kV). Detta skedde i början av ett fel i KGE, en buss bortom BFO. Båda dessa fall skedde när alla radialer var inkopplade och turbinerna producerade maximal uteffekt. Den högsta överspänningen inne i parken var 1,65 pu (44,45 kV) och observerades i början av ett trefasfel i KGE när alla radialer var inkopplade och turbinerna gick i tomgångsdrift. Den maximala överspänningen för varje konfiguration av Lillgrund inträffade på turbinen längst ut på den längsta radialen.

De högsta observerade överspänningarna på huvudtransformatorn var 1,56 pu (42,03 kV) på lågspänningssidan och orsakades av ett trefasfel i KGE, samt 1,17 pu (131,9 kV) på transformatorns högspänningssida, orsakat av ett tvåfasfel i BFO.

Den djupaste underspänningen registrerades på turbin E-02 med 0,014 pu (0,38 kV) kvarvarande spänning och orsakades av ett trefasfel i BFO. Detta skedde när endast en radial var ansluten.

Parkens effektgenerering samt antalet anslutna radialer påverkar över- och underspänningsnivåerna. Lägre effektgenerering resulterar i högre överspänningar samt djupare underspänningar på turbinerna. Färre anslutna radialer resulterar också i lägre överspänningar samt djupare underspänningar.

Contents

Abbreviations

PSCAD/EMTDC	Power Systems Computer Aided Design/
	Electromagnetic Transients including Direct Current
PSS/E	Power System Simulator/Engineering
HVDC	High Voltage Direct Current
RMS	Root Mean Square
PCC	Point of Common Coupling
FRT	Fault Ride-Through
SvK	Svenska Kraftnät
UMEC	Unified Magnetic Equivalent Circuit
STRI	Swedish Transmission Research Institute
PTI	Power Technologies International
PEN	Protective Earth Neutral
ABB	ASEA Brown Boveri
TN-C-S	Terra Neutral Common Seperate
SLG	Single Line to Ground
LL	Line to Line
pu	Per Unit
LV	Low Voltage
HV	High Voltage
TRF	Transformer
SCADA	Supervisory Control And Data Acquisition

1 Introduction

Lillgrund wind farm (Lillgrund) has been in operation for about a year. During this period of time it has been subjected to two commonly occurring faults in the 130 kV grid, owned by E.ON. One of these faults was a two phase short circuit fault, caused by colliding overhead lines and the other fault was a one phase to ground fault due to a lightning strike at the overhead line. Neither one of these faults caused any wind turbine to trip inside the farm, while other production units close by were affected. No data within the wind farm was recorded at the time of the faults since this is not possible to obtain from the SCADA system (the Siemens PAS version used at Lillgrund). In the 130 kV grid, data from transient fault recorders located at different locations was obtained.

A fault in the system can cause a severe voltage dip on one or more phases which then propagates in the grid. As the voltage dip propagates, it loses some of its magnitude due to the characteristics of transmission lines, cables and transformers between the fault location and the generators in the system. Even if the voltage dip is not that severe at the generator terminal, the generator is sensitive to small changes in the voltage. When faults upstream in the connecting grid causes a voltage dip, it is a demand that the wind farm will remain in operation. This property is called fault ride through (FRT) and is an important factor for the stability of the grid.

To learn more about how Lillgrund and future wind farms will respond to faults in the connecting grid, a simulation study was suggested by both E.ON and Vattenfall. For the simulation study, PSCAD/EMTDC was selected as the simulation software. An improvement of an existing PSCAD/EMTDC model of Lillgrund and the connecting 130 kV grid owned by E.ON was suggested to be developed in the software. This was to be done by using recorded data from the two faults in the 130 kV grid along with technical information about Lillgrund and the connecting grid, provided by both E.ON and Vattenfall. This study is financed by Vattenfall Vindkraft AB in cooperation with Vattenfall Power Consultant within the "Pilot Project Lillgrund" and is performed at Vattenfall Power Consultant in Göteborg, department Vindkraft.

A previous simulation study regarding balanced faults in the connecting 130 kV grid using a simplified model of Lillgrund has been performed by Vattenfall Power Consultant. This simulation study indicates lower levels of over voltages at Lillgrund than the insulation coordination study, performed by the manufacturer before the construction of Lillgrund wind farm.

An extended version of this thesis work will be handed out to Vattenfall Power Consultant, including plots from all performed simulations. This version can then be used to see whether the obtained results tend to be similar to the insulation coordination study results or the results from the previously performed simulation study by Vattenfall Power Consultant, if needed.

1.1 Previous Work

Previously performed analysis within areas concerning this project are mainly about system grounding, transient analysis and PSCAD/EMTDC modeling. Useful information about FRT capability for wind farms along with investigations on how different types of faults transpose through a transformer are to be found in the master thesis work by J. Enquist called "Ride-through of Offshore Wind Parks" [1]. In it, he examines how different grounding of transformers affect the FRT capabilities and gives recommendations for both wind turbine manufacturers and grid designers. Another useful report about grounding is the master thesis by J. Olsson and C. Hermansson "Nollföljdsmodellering av transformatorer - Beräkningar av följdproblem vid ökad kablifiering på mellanspänningsnivå" [2] (Zero sequence modeling of transformers - Consequences due to more cable installations on the medium voltage level) where zero sequence modeling of transformers is handled.

The article "Parameter Determination for Modeling System Transients - Part II: Insulated cables" by B. Gustavssen, J. A. Martinez and D. Durbak is very useful when modeling cables in PSCAD/EMTDC [3].

The engineers at Vattenfall Power Consultant have performed studies in PSCAD/EMTDC in cooperation with Chalmers University of Technology.

The manufacturer of Lillgrund wind farm has performed pre-studies which are internally accessible within Vattenfall.

1.2 Aim

Simulations are the only way to determine the fault response at Lillgrund since the SCADA system (Siemens PAS version used at Lillgrund) does not store any recorded data. The aim of this thesis is to simulate the transient response at Lillgrund due to faults in the connecting 130 kV grid. Most importantly is to determine dimensioning fault types and their applied locations, which causes extreme over and under voltage magnitudes at the main transformer and the turbines. The simulations will be performed using different amount of generated power along with different configurations of connected radials and different fault types. Based on these simulations, conclusions regarding the dimensioning fault types and their locations in the 130 kV grid will be made.

Moreover, a model of the 130 kV grid adjacent to Lillgrund will be developed in PSCAD /EMTDC using technical information provided by E.ON and Vattenfall. A model of Lillgrund, previously developed in PSCAD/EMTDC by Vattenfall Power Consultant will also be improved. This model should include controllable current sources to represent the turbines, instead of constant ones which were used previously. This will in a better way represent the behaviour of the full power converters used at Lillgrund. The current sources should deliver a constant active output power until a current limit of 1.4 pu is reached. After this, the active power output should decrease linearly as the voltage at the terminals drops. The two models will include frequency dependent (phase) cable and transmission line components within PSCAD/EMTDC, for increased accuracy.

1.3 Delimitations

This work is limited by the amount and accuracy of data that has been possible to obtain.

In the grid model that is developed in PSCAD/EMTDC, the HVDC connection is modeled as a current source. A better model of this connection would have been preferred but is beyond the scope of this work.

Due to the huge amount of data obtained from the simulations, not all possible correlation of data will be performed.

The ability to produce reactive power and hence keep the voltage up has not been taken into account in the turbine model. A better model of a full power converter which is able to control the phase angle is needed for this.

No relevant settings of the protection relays used at Lillgrund have been possible to obtain, which means that the FRT capability of Lillgrund will not be determined.

Frequency scans are not performed due to lack of data to compare the results with.

2 Power System Simulation Tools

Power system simulations can be done in a number of ways, all depending on the goal and objective of the simulation. These simulations can generally be divided into three different types:

- phase vector (steady state)

- electromechanical (time domain)

- electromagnetic (time domain)

Different companies have developed a number of softwares for different purposes. A short description of some of the most common ones will follow. All of them have the possibility to build custom model blocks.

2.1 PSS/E

PSS/E stands for Power System Simulator/Engineering and is mainly used for system studies. It can perform both phase vector and electromechanical simulations and has become one of the most commonly used softwares within the power system industry. Most wind turbine manufacturers provide PSS/E models that are e.g. used for verification of grid codes. PSS/E is developed by Siemens Power Technologies International (PTI).

2.2 Simpow

Simpow features all three types of simulations, phase vector simulation, electrodynamic and electromagnetic simulation. It was initially developed by ABB for simulations of HVDC but from 2004, STRI has taken over the copyright, development and marketing of the software.

2.3 DIgSILENT PowerFactory

DIgSILENT PowerFactory offers both stationary and transient simulations, as well as the library with the largest amount of pre-defined blocks used for wind power applications due to a cooperation with Risø University of Technology in Denmark.

2.4 PSCAD/EMTDC

Power System Computer Aided Design/Electromagnetic Transient including Direct Current is a simulation software that is mainly suited for electromagnetic simulations. PSCAD is the graphical interface and EMTDC is the simulation engine. The software can be used to model all parts of a power system, such as power electronics, motors and generators, connections, safety equipment, transformers etc. It is developed and distributed by Manitoba HVDC Research Centre. Vattenfall Research and Development is modeling the wind turbines at Lillgrund in this software and it is also used at Chalmers University of Technology, which Vattenfall Power Consultant has a collaboration with. The engineers at Vattenfall Power Consultant consider this to be the most suitable software for this type of simulations and was therefore chosen as the software for this project.

3   Regulations and Theory

For large wind farms such as Lillgrund with a nominal active power of more than 100 MW, there are some regulations regarding its capability to remain in operation due to different events occurring in the connecting grid that have to be fulfilled. These events could be faults which causes high fault currents and hence voltage dips. Before the regulations will be dealt with in section 3.2, some useful information about voltage dips will be presented in section 3.1. Useful theory about how different types of faults and grounding systems affect the currents and voltages in the grid during a fault will be presented in sections 3.3 and 3.4.

3.1   Voltage Dips

The following section has been inspired by the compendium "Power Quality and Electromagnetic Compatibility" [4] by Math Bollen and Ambra Sannino and deals with the definition and the characteristics of a voltage dip. Due to the subject of this report, only voltage dips related to faults will be in focus.

A voltage dip in the system is a reduction of the voltage, compared with the nominal RMS voltage for a short period of time. Different events such as short circuits and starting of large motors cause these voltage dips. The term "dip" is used interchangeable with the term "sag", which is preferred in the US.

3.1.1   Definitions

There is no clear definition of a voltage dip when it comes to magnitude and duration, different standards give different definitions. According to standard IEEE Std 1159-1995 [5], a voltage dip is a reduction of the voltage between 0.1 pu and 0.9 pu, compared to the nominal RMS voltage for a duration of 0.5 cycle to 1 minute at normal power frequency. The standard EN 50160 [6] defines a voltage dip as a reduction of the voltage between 0.01 pu and 0.9 pu, compared to the the nominal RMS voltage for a duration of 0.5 cycle to 1 minute.

3.1.2   Characteristics of Voltage Dips

A fault in the system can cause a severe voltage dip on one or more phases at the fault location which then propagates in the grid. As the voltage dip propagates in the grid, its magnitude will decrease, due to the characteristics of transmission lines and transformers between the fault location and the generators in the system. The high fault current produces high voltage drops over the impedances upstream in the grid, which limits the voltage drop and hence the voltage drop at the generator terminal will be less severe than close to the fault location [4]. It is desirable that the generators do not trip due to voltage dips.

From the Point of Common Coupling (PCC), the voltage drop will propagate undisturbed downstream in the grid towards the load terminals at lower voltage levels, affecting customers. This is the case when there is no generation connected to the low voltage level

which can keep the voltage level up [4].

When calculating the voltage level at different points in the system for unbalanced faults, sequence components are used. In section 3.3, the unbalanced fault types chosen for simulations will be investigated using this method. When analyzing balanced faults, a simplified voltage divider model for a radial system may be used. Such a model is seen in Figure 3.1, where the voltage level at the PCC is analyzed for a balanced three phase fault.
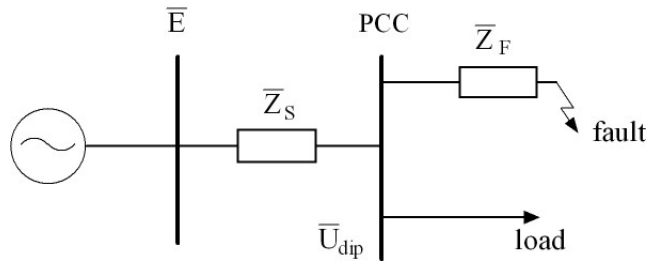

Figure 3.1 Voltage divider model.

The voltage source is a Thevenin equivalent with a no load voltage E and a source impedance Z_s, characterizing the network before the PCC. The feeder Z_F is modeled with a large value if the fault location is far away from the PCC and with a low value if the fault location is close to the PCC. The voltage U_{dip} at the PCC is then calculated using (3.1), with the assumptions that the load current is neglected before and during the fault and that the pre-fault voltage at the PCC is 1 pu.

$$U_{dip} = \frac{Z_F}{Z_S + Z_F} \tag{3.1}$$

This indicates that a voltage dip will be more severe if the fault is located close to the PCC i.e. a small value of Z_F or if the value of Z_s is large, characterizing a week network. The magnitude of the voltage dip will not differ much from the pre-fault voltage of 1 pu, if a transformer, characterized by a high impedance is located between the fault location and the PCC [4].

The duration of the fault is also characterizing the voltage dip, which is dependent on the fault clearing time of the protection used in the system. Faults in the transmission system are normally cleared much faster than faults in the distribution system due to stability issues [4].

3.2 Grid Codes

For large power production units with a nominal active power of more than 100 MW, there are some interconnection and operational requirements that have to be fulfilled, which are called grid codes. These grid codes are given by the transmission system operatator Svenska kraftnät (SvK), operating the Swedish national electrical grid which consists of the 200 kV and 400 kV lines plus installations and interconnectors to neighbouring countries.

Their duties include the responsibility for the electricity system being in a short-term state of balance and its installations working together in an operationally reliable way [7].

According to the publication "Affärsverket svenska kraftnäts föreskrifter och allmänna råd om driftsäkerhetsteknisk utformning av produktionsanläggningar SvKFS 2005:2" [8] (The Business Agency Svenska kraftnät's regulations and general advices concerning the reliable design of production units) there are some general demands on technical installations of a production unit that have to be fulfilled. The ones of interest for large wind farms will be presented in the following sections.

3.2.1   Tolerance Against Stationary Disturbances in Voltage and Frequency

Large wind farms should be able to deliver a certain amount of power, for different stationary variations in voltage and frequency according to Table 3.1. The voltage percent is relative to the nominal voltage at the wind turbine, converted to the highest voltage level of the system with consideration to the voltage drop during maximum active power production. See also Figure C.2 in Appendix C for a graphic presentation, using the figure notes in Table 3.1. For a short term voltage variation in one or more phases at the nearest meshed point of the national electrical grid according to Figure 3.2, large wind farms should be able to remain in operation. This voltage profile corresponds to an unsuccessful disconnection of a short circuit fault in the national grid, followed by a secondary disconnection by a breaker protection relay. The slow voltage rise after 250 ms is due to e.g. the magnetization of induction machines which requires reactive power. The lower voltage level after 700 ms is due to a weaker grid configuration after the disconnection of a line, which will result in a higher voltage drop in the remaining grid configuration than the pre-fault grid configuration [9]. For voltage transients due to common events in the net such as lightning strikes or operation of circuit breakers, large wind farms have to remain in operation.
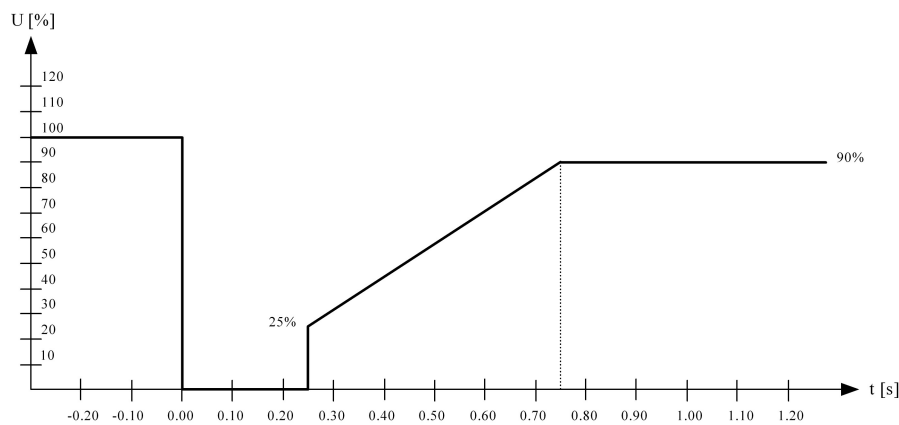

Figure 3.2 Short term voltage variation in the meshed transmission grid.

Table 3.1 Tolerance against stationary disturbances.

Frequency [Hz]	Voltage	Delivered power	Operational time	Notification	Fig
47.7-49.7	90-110%	No demands	10 min	Should be able a couple of times	
47.5-49.0	95-105%	< 5% reduction	> 30 min		a
49.0-49,7	90-105%	unchanged	continuous		b
49.7-51.0	85-90%	< 10% reduction	> 1 hour	Not for wind power plants	c
	90-105%	unchanged	continuous		d
	105-110%	< 10% reduction	> 1 hour		e
51.0-52.0	95-105%	reduced	> 30 min	When frequency is < 50.1 Hz, production has to return to normal within 1 min	f

3.2.2   Voltage Control

Large wind farms should be equipped with automatic voltage control that could control the voltage level within ± 5 % of the nominal voltage level. A control system which is able to set the exchange of reactive power in the PCC to zero, must be implemented.

3.2.3   Power Control

Disconnection of a large wind farm due to strong wind as well as connection of the wind farm to the grid, is not allowed in steps of more than 30 MW/min. Individual settings for each generator regarding the level when it is disconnected from the grid due to external impact must be implemented. It must be possible to set a maximum power production limit of the wind farm. This limit has to be controllable by using an external signal if needed. A reduction of the power production by external control due to problems in the connecting grid, must be fast enough to reach a limit below 20 % of maximum power production within 5 s [10].

3.2.4 Communication and Controllability

Real time information about voltage level, active power generation, reactive power exchange, operational status and controllability has to be carried out in such a way that it is available to SvK, if needed. If the normal operation is subjected to a disturbance, availability of manual operation within 15 min by remote control or by local control has to be implemented. The manual operation will include disconnection or connection to the grid, control of active power and reactive power i.e. to control the set point.

3.2.5 Verification and Documentation

For all demands given in SvKFS 2005:2 [8] valid for large wind farms, there have to be verifications. Different ways to perform verifications are full-scale tests, technical calculations, simulations and relay setting schedules. The design of a wind farm and all devices included, has to be documented. Relevant data in the documentation according to SvKFS 2005:2 has to be accessible to SvK, if needed. If changes are made in the technical documentation, they have to be reported to SvK.

The verifications of Lillgrund were performed by simulations, using the software PSS/E.

3.3 Unbalanced Fault Theory

This section has been inspired by [2], [11], [12]. Faults in the grid may have different causes and thereby different characteristics. Each fault may cause different kinds of stresses on the grid components, both over and under voltages. Balanced three phase faults are among the least common ones but cause the most severe voltage dips while single line to ground faults are the most commonly occurring ones, 70-90 % [13]. as well as the most dangerous ones for personnel.

Unbalanced faults of interest for simulations will be explained using symmetrical components. Theory regarding this method will not be explained, but is to be found in books about fault theory, such as "Power System Analysis and Design" [14]. The circuit used for the fault analysis is shown in Figure 3.3. From now on, phase currents during faults will

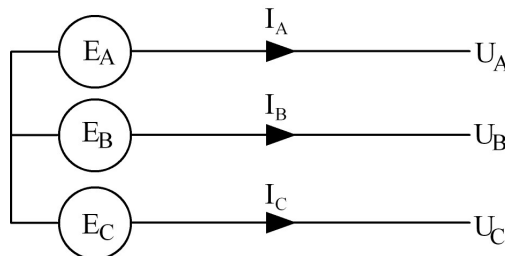**Figure 3.3** The pre-fault circuit used for fault analysis.

be denoted as I_A, I_B, I_C and sequence currents as I_1 (positive), I_2 (negative), I_0 (zero). The same applies for voltages, but with U instead of I. Pre-fault voltages are denoted

with E. For phase currents,

$$
\begin{aligned}
I_A &= I_1 + I_2 + I_0 \\
I_B &= a^2 I_1 + a I_2 + I_0 \\
I_C &= a I_1 + a^2 I_2 + I_0
\end{aligned}
\tag{3.2}
$$

applies and

$$
\begin{aligned}
I_1 &= \frac{1}{3}(I_A + a I_B + a^2 I_C) \\
I_2 &= \frac{1}{3}(I_A + a^2 I_B + a I_C) \\
I_0 &= \frac{1}{3}(I_A + I_B + I_C)
\end{aligned}
\tag{3.3}
$$

for sequence currents. Phase A is chosen as reference, resulting in $E_1 = E_A$ which is the voltage in phase A at no-load. Thevenin equivalents of the sequences are shown in Figure 3.4 and

$$
\begin{aligned}
U_1 &= E_1 - Z_1 I_1 \\
U_2 &= -Z_2 I_2 \\
U_0 &= -Z_0 I_0
\end{aligned}
\tag{3.4}
$$

are obtained from there.
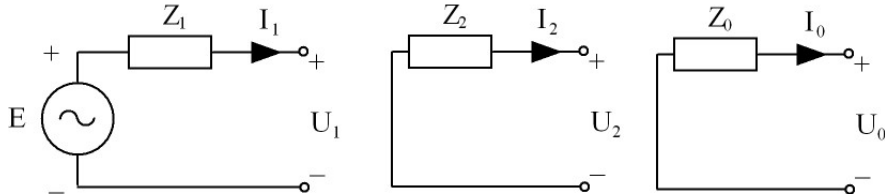
Figure 3.4 The Thevenin equivalent of the three sequence setups.

3.3.1   Single Line to Ground Fault

When doing fault analysis, the system is assumed to be in no-load. Upon application of the fault through a fault impedance Z_F, the following boundary conditions apply:

$$
\begin{aligned}
U_A &= Z_F I_A \\
I_B &= I_C = 0
\end{aligned}
$$

The network representation of a single line to ground fault is shown in Figure 3.5. That results in the sequence currents being

$$
I_1 = I_2 = I_0 = \frac{E_1}{Z_0 + Z_1 + Z_2 + 3Z_F}.
\tag{3.5}
$$

By using (3.4), (3.5) and the transformation matrix of the component theory, the phase voltages

$$
\begin{aligned}
U_A &= E_1 - \frac{Z_1 + Z_2 + Z_0}{Z_1 + Z_2 + Z_0 + 3Z_F} E_1 \\
U_B &= a^2 E_1 - \frac{a^2 Z_1 + a Z_2 + Z_0}{Z_1 + Z_2 + Z_0 + 3Z_F} E_1 \\
U_C &= a E_1 - \frac{a Z_1 + a^2 Z_2 + Z_0}{Z_1 + Z_2 + Z_0 + 3Z_F} E_1
\end{aligned}
\tag{3.6}
$$

and phase currents

$$
\begin{aligned}
I_A &= 3I_0 = \frac{3E_A}{Z_1 + Z_2 + Z_0 + 3Z_F} \\
I_B &= I_C = 0.
\end{aligned}
\tag{3.7}
$$

are obtained. If the fault resistance is zero ($Z_F = 0$), positive and negative sequence
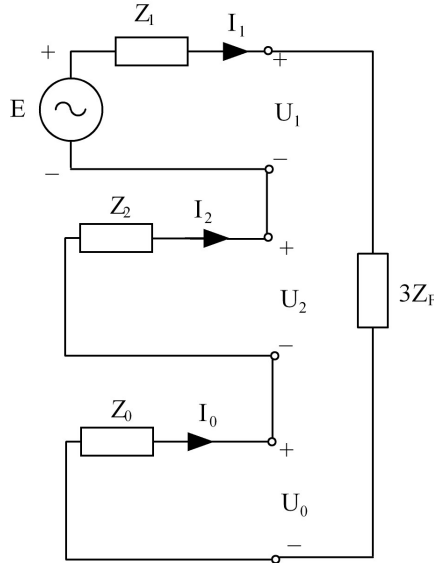
Figure 3.5 Sequence network for a single line to ground fault.

impedances are equal ($Z_1 = Z_2$) and the zero sequence impedance is large, (3.6) can be shortened to

$$
\begin{aligned}
U_A &= 0 \\
U_B &= a^2 E_1 - \frac{Z_0 - Z_1}{Z_0 + 2Z_1} E_1 = (a^2 - 1)E_1 = E_1\sqrt{3}\angle -150° \\
U_C &= a E_1 - \frac{Z_0 - Z_1}{Z_0 + 2Z_1} E_1 = (a - 1)E_1 = E_1\sqrt{3}\angle 150°
\end{aligned}
\tag{3.8}
$$

which shows that the highest obtainable phase voltage is line-to-line voltage.

3.3.2   Line to Line Fault

A line to line fault occurs when two lines are short circuited. As illustrated in Figure 3.6, the short circuit is through a fault impedance Z_F and the currents I_B and I_C are opposite to each other. The system is once again assumed to be in no-load, so the following boundary conditions apply:

$$
\begin{aligned}
U_B - U_C &= Z_F I_B \\
I_A &= I_B + I_C = 0
\end{aligned}
$$

The sequence representation of the faulted circuit is shown in Figure 3.7, where $E_1 = E_A$.
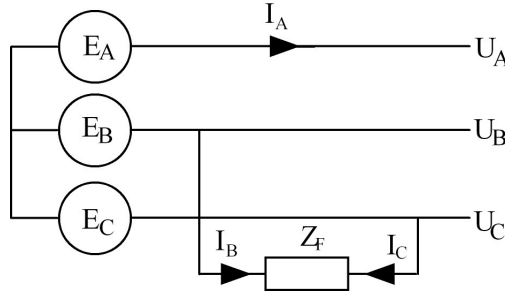
Figure 3.6 A short circuit between two phases through a fault impedance Z_F.

That results in the sequence currents being

$$
\begin{aligned}
I_1 &= -I_2 = \frac{E_1}{Z_1 + Z_2 + Z_F} \\
I_0 &= 0
\end{aligned}
\tag{3.9}
$$

and voltages

$$
\begin{aligned}
U_1 &= E_1\left(1 - \frac{Z_1}{Z_1 + Z_2 + Z_F}\right) \\
U_2 &= -Z_2 I_2 = E_1\frac{Z_2}{Z_1 + Z_2 + Z_F} \\
U_0 &= -Z_0 I_0 = 0.
\end{aligned}
\tag{3.10}
$$

By using (3.2) along with the relations $E_A = E_1$, $E_B = a^2 E_1$ and $E_C = a E_1$, the phase currents and voltages are obtained in

$$
I_B = -I_C = (a^2 - a)I_1 = \frac{E_B - E_C}{Z_1 + Z_2 + Z_F}
\tag{3.11}
$$

and

$$
\begin{aligned}
U_A &= E_A\left(1 - \frac{Z_1 - Z_2}{Z_1 + Z_2 + Z_F}\right) \\
U_B &= E_B - \frac{Z_1 E_B - Z_2 E_C}{Z_1 + Z_2 + Z_F} \\
U_C &= E_C - \frac{Z_1 E_C - Z_2 E_B}{Z_1 + Z_2 + Z_F}.
\end{aligned}
\tag{3.12}
$$
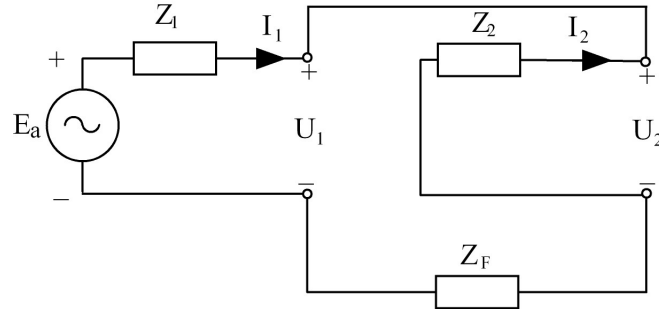
Figure 3.7 A sequence representation of a line to line fault.

These equations apply for all line to line faults. As can be seen, they can be thoroughly simplified to

$$I_B = -I_C = \frac{E_B - E_C}{2Z + Z_F} \tag{3.13}$$

and

$$
\begin{aligned}
U_A &= E_A \\
U_B &= E_B - Z\frac{Z_1 E_B - Z_2 E_C}{2Z + Z_F} = E_B - ZI_B \\
U_C &= E_C - Z\frac{Z_1 E_C - Z_2 E_B}{2Z + Z_F} = E_C - ZI_C
\end{aligned}
\tag{3.14}
$$

if $Z_1 = Z_2 = Z$ is assumed. That is the case unless the fault occurs close to machines.

The assumption means that the positive sequence impedance is used as the phase impedance on all phases, resulting in the circuit in Figure 3.8. Due to both Z_F and Z being induc-
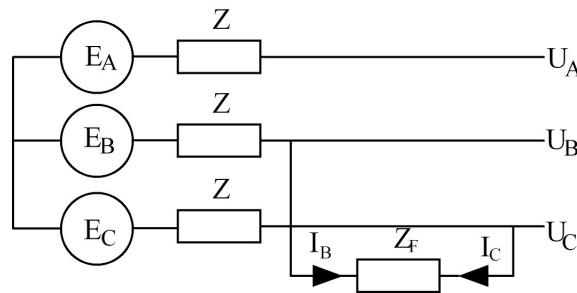
Figure 3.8 Simplified circuit of a line to line fault.

tive but Z having a larger impedance angle, the phasor diagram has the appearance as in Figure 3.9a at the fault location. A common assumption is a short circuit between phases, which means that $Z_F = 0$. The current equation then becomes

$$I_B = -I_C = \frac{E_B - E_C}{2Z} \tag{3.15}$$

13
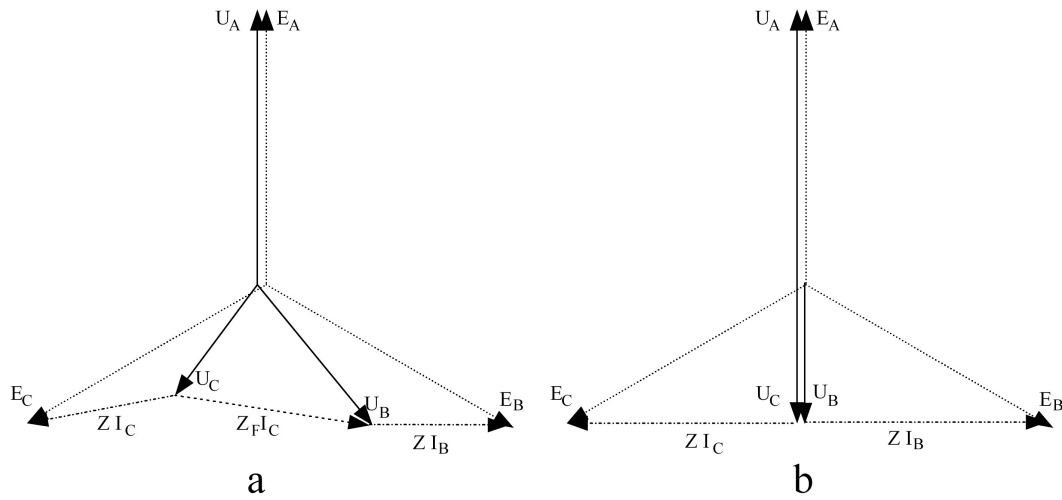
Figure 3.9 The phasor diagrams for a line to line fault where a) has a non-zero and b) zero fault impedance Z_F.

and the voltage equations are significantly reduced to

$$
\begin{aligned}
U_A &= E_A \\
U_B &= U_C = \frac{1}{2}(E_B + E_C) = -\frac{1}{2}E_A.
\end{aligned}
\tag{3.16}
$$

The phasor diagram has then the appearance as in Figure 3.9b.

Seeing that as a first estimation, it means that the voltages on the faulted phases become equal in both phase and amplitude at the fault location.

3.4   Grounding Theory

Grounding of systems has a number of benefits. One is that the system can be divided into a number of subsystems without interconnected zero sequences, another is that the fault current can be limited and a third that it is necessary for the safety of personnel.

When doing the following analysis, the fault impedance Z_F is assumed to be 0, and $Z_1 = Z_2 = Z$, which gives

$$
I_A = \frac{3E_A}{2Z + Z_0}
\tag{3.17}
$$

from (3.7).

In (3.17) it is possible to see what parameters affect the fault current. The parameter that can most easily be changed is the zero sequence impedance, which is greatly dependent on the grounding impedance. The grounding impedance is then set in a way that could limit the fault current if desired.

3.4.1   Solid Grounding

Solid grounding of a system, means that the neutral is directly connected to ground, as shown in Figure 3.10. This type of grounding is safest for personnel although it results in high fault currents, sometimes higher for a single line to ground fault than for a three phase fault. The high current makes the fault easy to detect and clear quickly with regular over current protection, both at system level and in households. Another advantage of
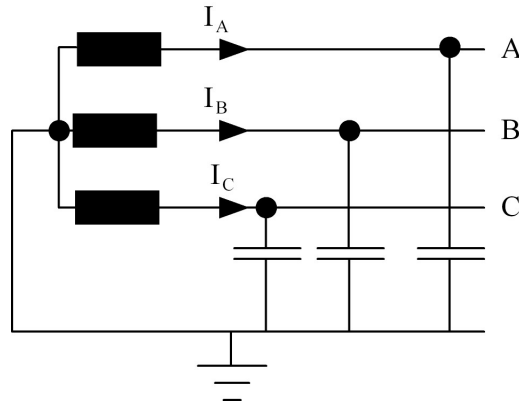
Figure 3.10 Circuit diagram of a directly grounded system.

this system is that the voltages on non-faulted phases change very little, which is why it is used in Sweden in all 130 kV and above transmission systems. A disadvantage is the difficulty of clearing highly resistive faults such as arcs to ground, resulting in longer over current times and risks of equipment damage [1].

3.4.2   Resistive Grounding

Resistive grounding is something in between an isolated and a directly grounded system. The neutral is connected to ground through a resistor, as shown in Figure 3.11 which is either low or high ohmic. The low ohmic grounding current limit is set to 2-4 [1] times the nominal current, so that the fault current can be distinguished from normal operational current. This system

- reduces burning and melting effects in faulted equipment.

- reduces arc blast or flash hazard to personnel in close proximity to the ground fault.

- prevents high touch and step voltages and transferred potentials.

- prevents interferences on secondary equipment.

- reduces the voltage dip in low voltage systems supplied by the low impedance grounded system during a ground fault.

- is used in the 30 kV cable grounding system of Lillgrund.

Figure 3.11 Circuit diagram of a resistively grounded system.

High ohmic grounding is used for obtaining a high operating reliability like in isolated systems but also to detect ground faults. There are two factors to consider when choosing the resistance of high ohmic grounded systems. One is the current limit, typically 5-25 A depending on the application and the other is that the resistive current needs to exceed the capacitive current for easier fault detection [1].

3.4.3   Reactive Grounding

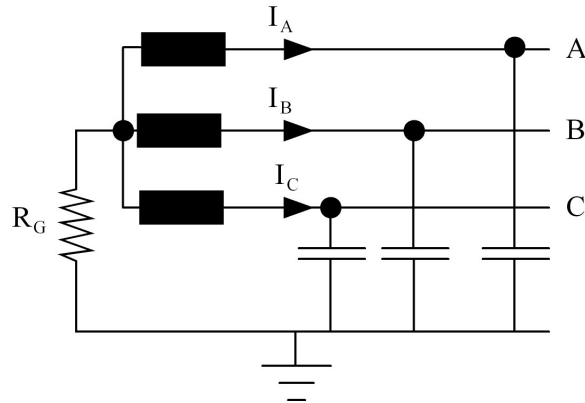Reactive grounding as shown in Figure 3.12 is done in order to reduce the capacitive current in the system. By tuning the reactor to the capacitance of the system, resonance is obtained and the reactive and capacitive currents even each other out. Although, due to resistive losses in the insulation illustrated with the resistance R in Figure 3.12, there will always be a small resistive current flow.

The advantage of this system is that it makes arcing faults to ground self extinguish because the current is low and in phase with the voltage. Therefore, protections only need to remove permanent faults.

3.4.4   Isolated Systems

Systems may also be isolated from ground, as shown in Figure 3.13. One reason for this is that the fault currents are limited in case of ground faults, according to (3.7) since $Z_0 \to \infty$. This, on the other hand, causes the voltage on the non-faulted phases to rise by $\sqrt{3}$ according to (3.8). The low fault current may be difficult to detect, causing the over voltage to remain over the insulation, stressing it further. Weak spots in the system, such as cable joints which are subjected to continuous over voltage are likely to break down, leading to another connection to ground, elsewhere in the system. Two simultaneous ground faults on different locations in the system cause large over currents and may lead to incorrect tripping of relays, thereby disconnecting non-faulted parts of the system [1].
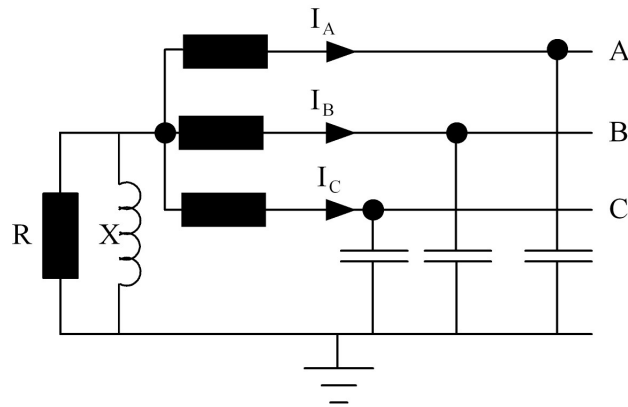
Figure 3.12 Circuit diagram of a reactively grounded system.
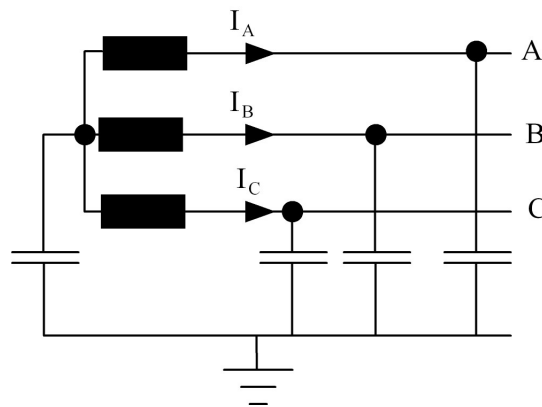
Figure 3.13 Equivalent circuit in an isolated system.

In the case of medium or low voltage networks, the insulation is commonly designed to withstand additional $\sqrt{3}$ of the nominal voltage, making the over voltage less of a problem, compared to higher voltage levels, where that is not the case. Since the voltage rises on the remaining phases, the line to line voltage towards the faulted phase remains unchanged. In cases like this, the system can keep operating even when faulted, meaning that this grounding system has a high operating reliability.

Due to the capacitive coupling to ground, shown in Figure 3.13, the system is not perfectly isolated, but the impedance is large enough to keep the current very small.

4   Lillgrund Wind Farm

Lillgrund is located about 10 km southwest of Malmö between Sweden and Denmark, as seen in Figure 4.1. The location was specifically chosen due to its average wind speed of 8-10 m/s and average water depth of 4-10 m [15].

Figure 4.1 Location of Lillgrund wind farm [16].

4.1   Technical Information About Lillgrund

Lillgrund is made up of 48 Siemens SWT-2.3-93 2.3 MW wind turbines, so its total installed capacity is 110 MW. Each turbine has a tower height of about 70 m and a rotor diameter of 93 m. They are equipped with induction generators behind full power converters, meaning that the active and reactive power outputs can be controlled independently of each other. The generators run internally on 0.69 kV and are connected to a 33/0.69 kV step up transformer rated at 2.6 MVA, placed at the bottom of the tower.

The turbines are connected to a 30 kV collecting grid in five radials going into the transformer platform, as can be seen in Figure 4.2. The cable thickness varies depending on the amount of current that needs to be carried.

18
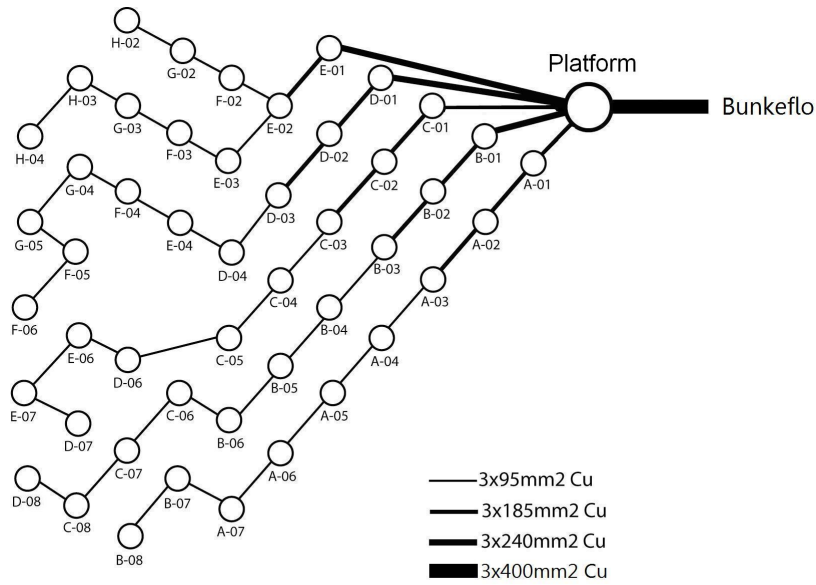
Figure 4.2 The collection grid illustrating the different cables.

The platform has a 30 kV switchyard and a 138/33 kV step up transformer rated at 120 MVA, which is slightly over dimensioned in order to increase its lifetime. The outgoing cable is operating at a high voltage to reduce the transmission losses and to minimize the number of outgoing cables [17]. The cable is then connected to the 130 kV grid at Bunkeflo substation. Figure 4.3 shows the simplified electrical sketch of Lillgrund and its different voltage levels.
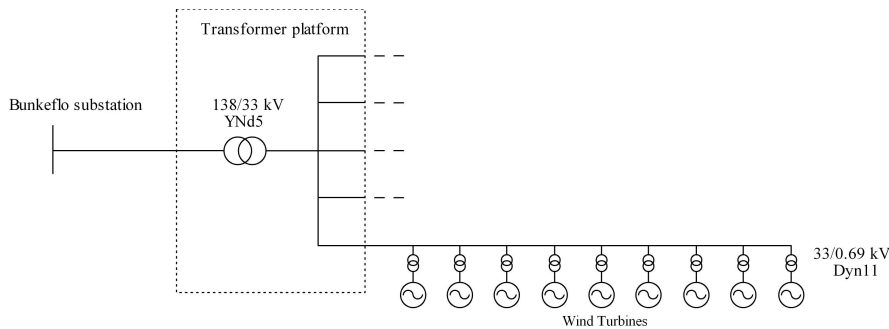
Figure 4.3 Simplified electrical sketch of Lillgrund wind farm.

The average yearly production is estimated to 330 GWh [15], which is an average power output of 37.7 MW or 34.2 % of the maximum capacity. Compared with other offshore wind farms, Lillgrund is below average according to Table 4.1.

Table 4.1 A comparison of different wind farms.

Wind Farm	Estimated Energy [GWh]	Installed Power [MW]	Estimated Average Power[1] [MW]	Efficiency [%]
Nysted Wind Park [18]	595	165.6	67.9	41.0
Horns Rev [19]	600	160	68.5	42.8
Princess Amalia [20]	435	120	49.7	41.4
Lillgrund [15]	330	110	37.7	34.2
Kentish Flats [21]	280	90	32.0	35.5
Burbo Bank [22]	315	90	36.0	40.0
North Hoyle [23]	200	60	22.8	38.1
Avg Efficency				**39.0**

4.2 Grid Performance Specifications

The following information is specified in a grid performance document [24] provided by Siemens Wind Power A/S concerning the FRT capability of a wind farm consisting of Siemens SWT-2.3-93 2.3 MW wind turbines.

The FRT capability due to a short term voltage variation in one or more phases at the nearest meshed point of the national electrical grid [25] is specified in Table 4.2. The voltage is relative to the pre-disturbance voltage of 1 p.u and the time is the maximum time that the wind farm will remain in operation as long as the voltage is reduced.

Table 4.2 FRT capability

Voltage [p.u]	0	0.15	0.75
Time [s]	0.25	0.65	10

These values are valid as long as the amount of installed wind turbines are in proportion to the strength of the grid. That is, the short circuit ratio (S_k/S_n) and the (X/R) ratio of the grid seen from the wind turbine terminal have to be adequate. Otherwise if the grid is not strong enough, the voltage will not recover adequately when the fault is cleared [26].

The normal voltage range at the low voltage side of the transformer located inside the turbine, is between 0.90 pu and 1.1 pu. For best performances and to stay well within operation limits, the range should be between 0.95 pu and 1.05 pu.

The operating frequency range is between 47 Hz and 52 Hz.

---

[1]The average power output of the farm based on the yearly production.

The specified values in Table 4.2 are to be compared to the voltage profile in Figure 3.2, which indicates that the demand given by Svk is fulfilled.

4.3 Grounding System at Lillgrund Wind Farm

There are in total three grounding systems used at Lillgrund, one for each voltage level. Even though there are three different systems for grounding they are all linked together by cable screens and earth electrodes placed on the foundations of the transformer platform and on the wind turbine platforms, forming a large meshed grid. In order to keep the different grounding systems separated in case of a fault in one grounding system, suitable transformer configurations have to be selected with no path for the zero sequence current to flow between the two sides of the transformer. This will prevent any protection relays on a non faulted voltage level to trip.

4.3.1 Grounding of the 130 kV System

In Sweden, the neutral point of the 130 kV system is directly connected to ground [27]. The reason for this is to minimize the voltage rise at the non faulted phases in case of a single line to ground fault and hence to keep the insulation level of the equipment in the system as low as possible [12]. This indicates why the grounding system on the high voltage side of the 138/33 kV transformer is also chosen to be directly connected to ground i.e. high insulation level means higher costs. The 138/33 kV transformer at the platform is connected as YNd5, which means that the neutral point at the high voltage side of the transformer is connected directly to ground and that there is no connection to ground on the low voltage side. By using this coupling, no zero sequence current will flow between the two sides of the transformer. Simplified zero sequence and positive sequence equivalent circuits of a YNd transformer are shown in Figure 4.4, where the representation of magnetization and core losses are neglected due to its high impedance [11]. For static components like a transformer, positive and negative sequence impedances are the same [11].
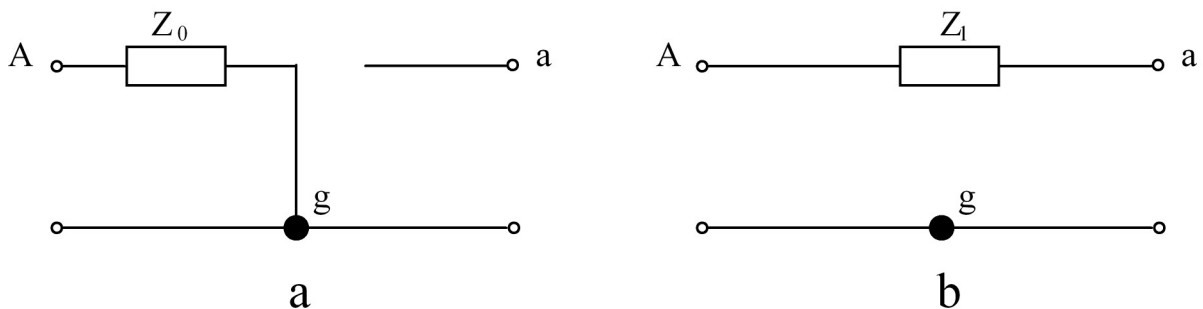

Figure 4.4 a) Zero and b) positive sequence circuit of a YNd transformer.

4.3.2 Grounding of the 30 kV System

The grounding system of the 30 kV system is built as a low resistance grounding system to limit the maximum earth fault current.

The windings on the low voltage side of the 138/33 kV transformer are connected in delta and hence there is no neutral point available for connecting the low resistance to ground. The same applies for the high voltage side of the transformers located at the wind turbines, which are also connected in delta. This problem is solved by using a stand-alone 33/0.4 kV earthing transformer at the platform connected as ZNyn5, where a neutral point is available for resistive system grounding, as seen in Figure 4.5. The transformer configuration also includes a low voltage winding for auxiliary supply at the platform. Each phase winding is split into two equal windings and then wound around
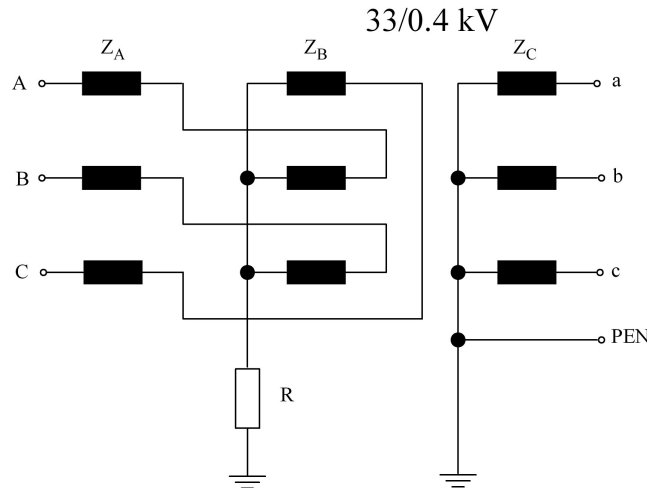
Figure 4.5 Configuration of a ZNyn transformer with resistive grounding.

two separate legs of the transformer. Hence there will be two windings on each leg from two different phases which will keep the voltage of the different phases at approximately the same level even if a unsymmetrical load is connected to the low voltage side. This is a great advantage for this kind of transformers [28].

By using a ZNyn5 transformer, the high voltage side will be separated from the low voltage side in the zero sequence equivalent circuit [29]. This indicates why this transformer configuration is used instead of a YNyn transformer, where the zero sequence current would have a path between the primary side and the secondary side of the transformer. The simplified zero sequence equivalent circuits of a ZNyn transformer and a YNyn transformer are shown in Figure 4.6.

4.3.3 Grounding of the 0.4 kV System

The grounding system of the 0.4 kV system used for auxiliary power supply at the transformer platform is operating as a TN C-S system. That is with the transformer neutral point directly connected to ground and a PEN conductor out of the transformer also
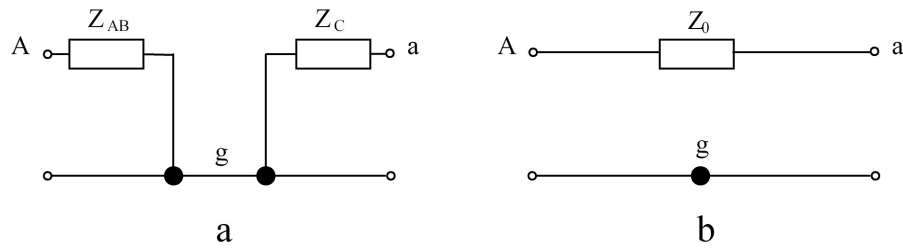
Figure 4.6 Zero sequence circuit of a a) ZNyn and a b) YNyn transformer.

connected to the neutral point, as seen in Figure 4.5. This is later split into separate PE and N conductors. In case of a fault, this will give a high short circuit current and hence trip any circuit breaker fast on the low voltage side, for safety reasons.

5   Modeling in PSCAD/EMTDC

PSCAD/EMTDC was chosen as the simulation tool because the engineers at Vattenfall Power Consultants consider it to be the most developed simulation tool for electromagnetic simulations. The software will in the future be referred to only as PSCAD.

In the upcoming section, some general information on how to model different types of components will follow and also how the modeling of Lillgrund and the connecting 130 kV grid was performed. How different assumptions when modeling have had an impact on the total accuracy and how this affects the results will be treated in section 5.5.

5.1   General Information about PSCAD Modeling

Because it is possible to model all system parts in PSCAD, a brief description of the modeling procedure of the used components will follow. The same procedure was followed during the construction of the models for this project.

5.1.1   Cables and Transmission Lines

The modeling of cables and overhead lines is done geometrically in PSCAD, which requires input parameters as shown in Figures 5.1a and 5.2. When it comes to cables, it is possible to have more layers than what appear in the figure, all depending on the type of cable that is modeled. These types of models make it possible to study reflections.

Figure 5.1 A general PSCAD cable model.

The first layer, between r0 and r1, in Figure 5.1a is the modeled conductor where r1 is the radius given in the datasheet and r0 is a correction done due to the conductor being stranded. This construction is needed due to the fact that PSCAD models the conductor
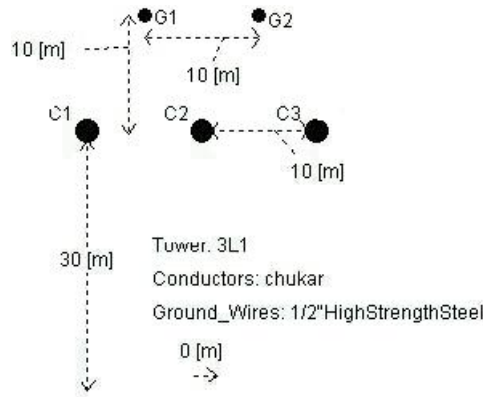
Figure 5.2 A tower model from PSCAD/EMTDC.

as solid, when it may be stranded in reality. The inner radius r0 is obtained from (5.1) [3].

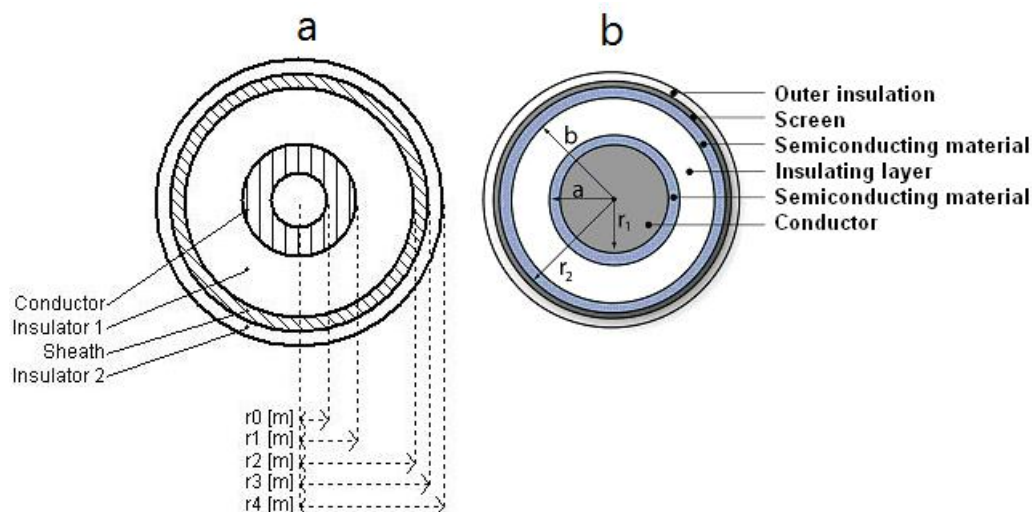$$r_0 = \sqrt{r_1^2 - \frac{A}{\pi}} \tag{5.1}$$

The second layer, between r1 and r2, represents the semiconducting layers and insulation. Since the semiconducting layer cannot be represented separately, they are taken into account by modification of the insulation permittivity. This modification is done according to (5.2) where $\epsilon_{r,ins}$ is the permittivity of the insulating layer and r_1, r_2, a and b are defined in Figure 5.1b [3].

$$\epsilon_r = \epsilon_{r,ins} \frac{ln\frac{r_2}{r_1}}{ln\frac{b}{a}} \tag{5.2}$$

Modeling of overhead lines is principally shown in Figure 5.2. This shows that the distances between wires and height above ground are some of the needed data. Wire radiuses and resistivities are also specified along with e.g. sag and transposition.

After the models have been created geometrically, they have to be stabilized. This means that their simulation settings have to be tuned so that EMTDC can perform finite numerical solutions. These settings are dependent on the simulation time step, cable/line length etc, which means that those parameters need to be decided before the stabilization process is started. This process can be time consuming.

5.1.2 Transformers

When EMTDC performs calculations on transformers, it does so on a detailed level by calculating the magnetic flux in the core [30]. The difference between models is the type of core used. Regular transformers treat the phases independently of each other while Unified Magnetic Equivalent Circuit (UMEC) transformers can be modeled as a three or five limb core. If a UMEC transformer is used, a part of the input data needs to be according to Figure A.1, while the right table is non-existent if transformer saturation is

disabled. All together, there is a good amount of models to choose from depending on the known parameters and the desired detail level. The Z_0 of the transformer depends on three main parameters, the leakage reactance, no-load losses and copper losses. These parameters are found in the test protocol for transformers.

5.1.3 Custom Model Blocks

It is also possible to create custom model blocks in PSCAD, in which case all available building blocks can be used. The models can be anything from whole grids to single generator or turbine models.

5.2 Wind Turbine Modeling

The wind turbine is modeled by using controllable current sources that delivers a constant active output power up to 1.4 pu of the nominal current as the voltage drops. This is implemented by defining a reference current for all three phases using a resistive reference circuit as seen in Figure 5.3.
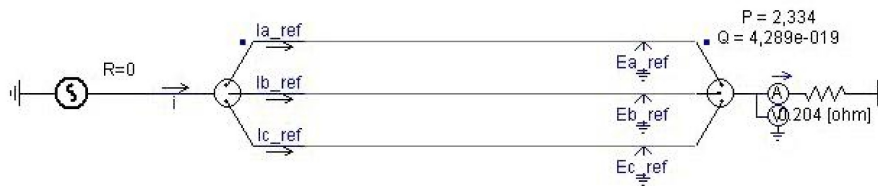
Figure 5.3 Current referent circuit.

The voltage is set to 0.69 kV at the terminals of the reference voltage source and the resistances are chosen so that the nominal active power of one wind turbine is consumed. The current Ia_ref drawn by the load in phase a is then measured and used as a reference current in the control system for the variable current source. The phase voltage Ea_ref is also measured and used as a voltage reference. The same process applies for the other two phases. The control system for phase a is seen in Figure 5.4.
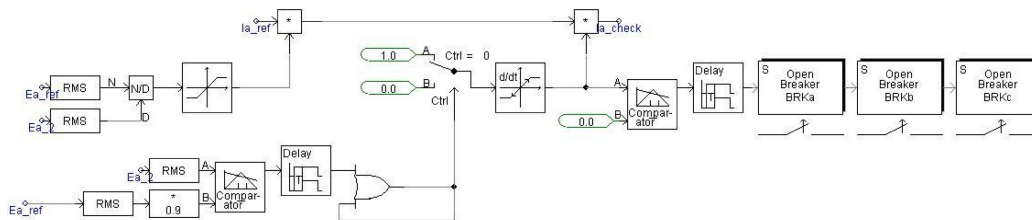
Figure 5.4 The wind turbine control system.

The RMS value of the reference voltage is compared with the RMS voltage value measured at the low voltage side of the 33/0.69 kV transformer placed at the bottom of the tower. The value of the ratio is then multiplied with the reference current. This current

26

is called *Ia_check* and will function as a input current to the controllable current source. The change in current will follow the voltage change at the terminal of the generator and hence keep the active power at the same level. A limitation of 1.4 in the voltage ratio is implemented to act like a current limiter. The reactive power generation is set by choosing a voltage angle of the reference voltage source. This will make the reactive power generation in each wind turbine equal and can not be set individually. The angle is chosen so that the exchange of reactive power in the PCC is as close to zero as possible during normal operation. During a fault, there is no automatic control of the phase angle implemented in the model. This means that the wind turbine model can not support the grid with reactive power and hence keep the voltage up during a fault. Reactive power support is usually a normal operation feature for a full power converter [31].

When the control system was developed, no relevant information was given by the manufacturer about the turbine performance specifications, other than that the normal operation range is between 0.9 pu and 1.1 pu of the nominal voltage level. The lack of information resulted in the assumption that when the voltage level was below 0.9 pu for one period, the active power would ramp down to zero and then the circuit breakers would open. This would effect all three circuit breakers even if the voltage dip only occurred in one phase. As no information about the turbine performance specifications was to be found, a decision was made to keep the model intact, but to set the low voltage comparator time far longer than the simulation time. This means that the current ramp down function and the circuit breakers are not in operation during simulations. The voltage level at the wind turbine during a fault will have to be compared to relevant data regarding the turbine performance specifications, for determination of the FRT capability of each turbine.

The 33/0.69 kV Dyn11 transformer at the bottom of the wind turbine tower is modeled by using a three limed UMEC transformer with pre-defined settings for saturation.

5.3 Modeling of the Collecting Grid

The cables in the collecting grid are modeled as frequency dependent (phase) cable models. The length and the sequence data of the cables were given in documents provided by the manufacturer. The lengths of the cables in the connecting grid are rather short, which required a very short time step. To avoid the problem that the signal would travel the whole cable length between two recorded samples, a time step of 2 μs was chosen. This short time step made the total simulation time extremely long.

The main 138/33 kV YNd5 transformer at the platform was modeled using a three limbed UMEC transformer including pre-settings for saturation. Transformer parameters were set according to transformer specification provided by Vattenfall [32]. The transformer zero sequence impedance (Z_0) is heavily dependent on the tap changer position, varying between 12.1 Ω/phase and 22.0 Ω/phase [33]. The tap changer was set to position 13 in the model, which is the rated voltage ratio position. This will give a zero sequence impedance of 15,1 Ω/phase. In the transformer model, the zero sequence impedance could not be specified explicitly.

The 33/0.4 kV ZNyn grounding transformer was modeled according to Figure 5.5, since no standard model of this transformer configuration is available in PSCAD.
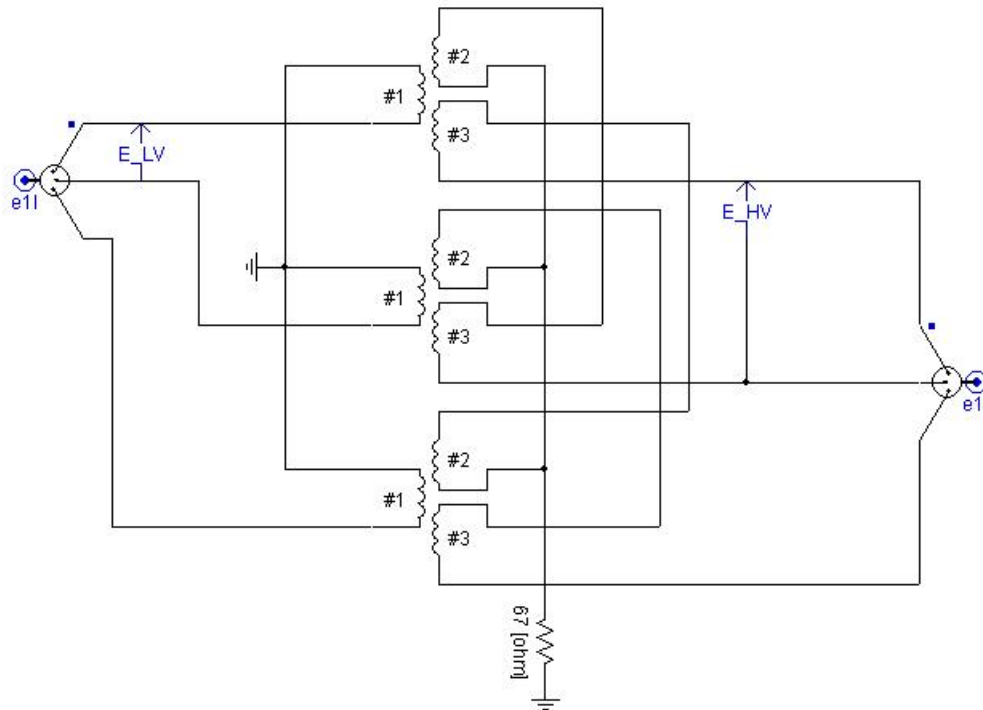
Figure 5.5 ZNyn-transformer.

Three single phase transformers, consisting of three windings each were used to implement the ZNyn configuration and the connection to the resistance, as seen in Figure 4.5. From the transformer rating plate the impedance voltage 2.02 % was given on a 150 kVA base along with the zero sequence impedance of 32.24 Ω. Since each single phase transformer used in the model is rated 50 kVA, the impedance voltage had to be divided by three. This value was then used as positive sequence reactance in the model. The magnetic coupling between the three phases are excluded in the model, since this could not be implemented. The transformer is modeled with no losses, which is assumed to have little effect on the simulation results since this transformer is used mainly as a current limiter due to faults within the 30 kV system. The 67 Ω grounding resistance together with the 32.24 Ω/ph zero sequence impedance according to Siemens documentation will limit the earth fault current to 300 A.

5.4 Modeling of the Connecting Grid

A single-line diagram of the 130 kV grid was provided by E.ON [34]. The diagram is shown in Figure 5.6 and represents the grid in the vicinity of Lillgrund and those parts of the grid where the faults of interest occurred. PI models of all connections and PSCAD models of some lines were also provided by E.ON [34]. PI models for the 400 kV connections

between BBK-SEE and SEE-AIE, along with the short circuit power for the connecting buses at BBK and SEE were provided by Vattenfall [35].
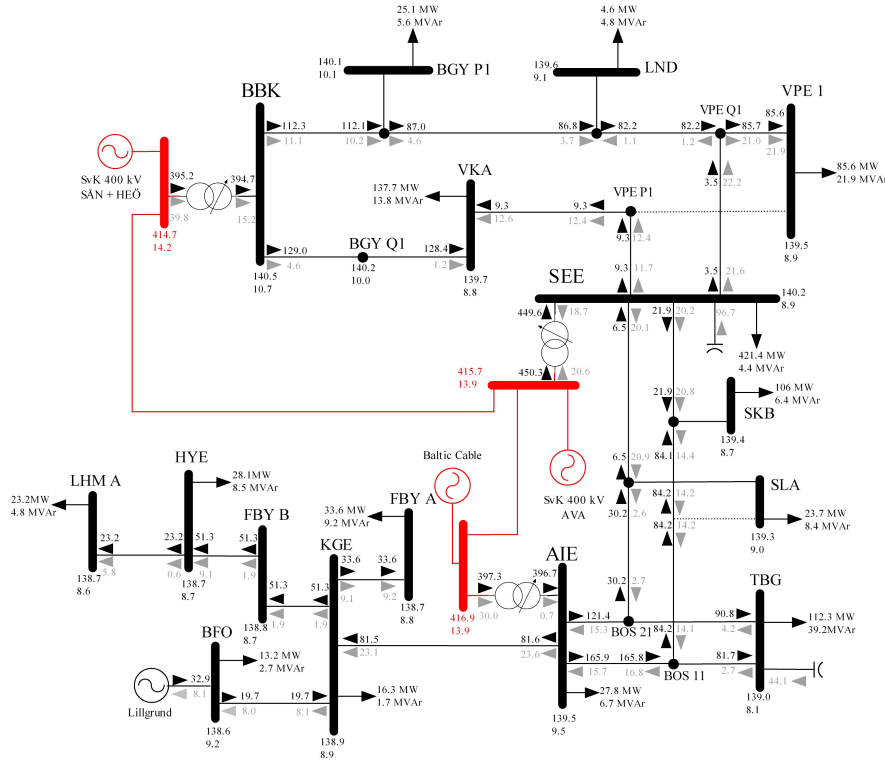
Figure 5.6 The obtained E.ON grid.

The load flows and the bus voltages in the provided diagram are from a highly loaded occasion sometime in January or February 2008 [36]. Due to lack of other information, this grid configuration was used during the transient verification despite the fact that the configuration may have been different in reality at the time of the faults. During the other simulations, only the power input from Lillgrund was changed for different cases which led to slight differences in the power flows and voltage levels.

The singe-line diagram did not specify the type of load connected to the different buses. According to E.ON [37] a reasonable assumption was to model half of the total load as constant impedances and the other half as constant power loads. This was implemented in the model by setting loads less than 10 MVA as constant impedances without transformer, loads between 10 MVA and 100 MVA as constant impedances with transformers and loads larger than 100 MVA were assumed to draw constant power, with some exceptions. The amount of load represented by a constant impedance is 650.65 MW and the load represented by constant power is 621.55 MW.

The transformer parameters were obtained for all needed 400/130 kV transformers and for three 130/50 kV transformers. Therefore, all transformers to voltage levels below 130 kV were assumed to be to 50 kV. One 130/50 kV transformer was from a substation outside the model and was only a few years old while the other two were from the 60s and

29

from substations included in the model. The parameters for all 130/50 kV transformers were therefore set to an average of the parameters of these two transformers. The large transformers were rated at 750 MVA and the small ones at 60 MVA. The ratings of transformers at loads larger than 60 MVA were adopted in order to fit the loads appropriately.

When it comes to the 400/130 kV transformers, two substations had two serial transformers, one for 410/145 kV transformation and one for the tap changer in series, while the third substation had one transformer that included a tap changer. For simplicity each substation was modeled with one transformer with the transformation ratio being equal to the voltages obtained in the E.ON. single line diagram.

The grounding resistance of all transformers was assumed to be 1 Ω.

As shown in Figure 5.6 the Baltic High Voltage Direct Current (HVDC) transmission connects to the AIE substation. In the load flow situation provided by E.ON, the HVDC transmission supplied the system with 400 MW. The first model of it was a voltage source which balanced itself to feeding approximately 410 MW and 200 MVAr. This was replaced with a current source defined to provide the same amount of power as the voltage source. The change was done because it was considered to be a more accurate representation [38] of a HVDC connection, but still a simplification. During faults in the grid, the HVDC link will contribute with current and power transients at fault inception and fault clearing. Due to the nonlinear characteristic of the HVDC link, these phenomena are not represented in the simplified model used in this report. These transients may occur when the voltage on the inverter side of the HVDC link drops below 0.95 pu for fully loaded HVDC transmissions. Less loaded transmissions can withstand deeper voltage dips [26] which means that the HVDC link should be less sensitive in this case because it is loaded to approximately 70 % of its maximum capacity of 600 MW [39]. During such faults, the current from the HVDC link is reduced to approximately 35 % of its nominal until the voltage is recovered, after which the current is ramped back to nominal within 100 ms.

EMTDC models were obtained for most connections. For the remaining connections, complementary sources were used to make appropriate models [40], [41]. The Eniro satellite photography [42] and map were also used to estimate the length of the line between BOS and TBG to 12 km and between HLP and SLA to 4 km.

5.5   Accuracy

Some details were missing when the PSCAD model was built, while other parts had to be simplified due to their complexity. Assumptions had to be made in order to obtain a model that was fast enough when performing the simulations, without losing too much accuracy.

Amongst the missing details are sources that connect to the 130 kV and below grid, the exact type of loads on all buses, correct modeling of the Baltic HVDC connection and the 130 kV transformer configurations.

Considering that the two 400 kV connecting buses SEE and BBK have a short circuit power of 1.8 GVA and 7.1 GVA respectively, the short circuit power contribution from sources connected to the 130 kV substations should not affect the total short circuit power contribution noticeably.

Since the HVDC connection is feeding power into the AIE substation, it is sensitive for under voltages because that increases the risk for commutation failures. If such failures happen, the power flow from the HVDC connection goes down to approximately 35 % during the fault but is restored after the fault is cleared [26]. Such a fault may have marginal consequences on this system because of the two strong connections that SEE and BBK are since they should be able to replace the power that is lost from the HVDC connection in case of a fault.

The distribution of the constant impedance loads is regarded as reasonable due to the small amount of industrial consumers in the area close to the Bunkeflo substation, which mainly consists of household consumers. In the area further away from the Bunkeflo substation, loads with constant power represent parts of the 130 kV grid that are not included in the model. These loads are modeled without a transformer due to this representation.

The load transformer configurations used in the model are simplified. For all transformers, the pre-set values for saturation are used since no information was obtained regarding their actual saturation parameters. The loss of accuracy due to this is assumed to be negligible [43].

Data of all transformers used in the model was not available which led to the previously mentioned modeling simplification. The parameters used for the 130/55 kV transformers in the model, will reduce the accuracy since these are not the actual parameters of the transformers. It is assumed that this will represent the transformers in an appropriate way. The loss of accuracy due to this is also assumed to be negligible.

The simplification used when modeling the 400/130 kV transformers by including the tap changer transformer in one transformer may affect the reactive power consumed by the transformers somewhat. This will affect the power flow slightly.

All simplifications and lack of information affects the total accuracy somewhat, but most are negligible.

6 Model Verification

The model has been verified in two ways, with load flow and fault response. The verification of the load flow was done through comparison of the simulated load flow and voltage levels with the ones acquired in the single-line diagram from E.ON. Measuring data from a transient fault recorder was used for fault response verification. Issues regarding differences between the simulated and measured response will be discussed in 6.4.

6.1 Load Flows and Bus Voltages

The first things observed were the voltages and power flows in the system. A maximum error of 10 % of the total power flowing into the system was set as an upper limit for the error at any bus [43]. Counting the total power flow into the system according to Figure 5.6 to 1275.8 MW, the maximum allowed deviation at any line was 127.58 MW. The maximum allowed voltage deviation was set to 5 %. The load flows and bus voltages of the connecting grid model are shown in Figure 6.7 and summed with the most important ones in Tables 6.1 and 6.2. As can be seen in the figure and tables, nothing deviates outside the set limits. From that point of view, the model is acceptable.

Table 6.1 Load flows in the PSCAD model, the E.ON model and the differences.

Line / Transformer	Active power flow [MW]		
	E.ON. PSS/E model	The PSCAD model	Deviation
BBK 400/130	394.7	390.4	-4.3
BBK-BGY P1	112.3	110.4	-1.9
BBK-BGY Q1	129	126.4	-2.6
SEE 400/130	449.6	446.3	-3.3
SEE-VPE P1	9.3	11.5	2.2
SEE-VPE Q1	3.5	6.1	2.6
SEE-SLA	-6.5	-9.6	-3.1
SEE-SKB Q1	21.9	19	-2.9
AIE 400/130	396.7	400.5	3.8
AIE-KGE P1	81.6	81.8	0.2
AIE-BOS 21	121.4	122.6	1.2
AIE-BOS 11	165.9	167.5	1.6
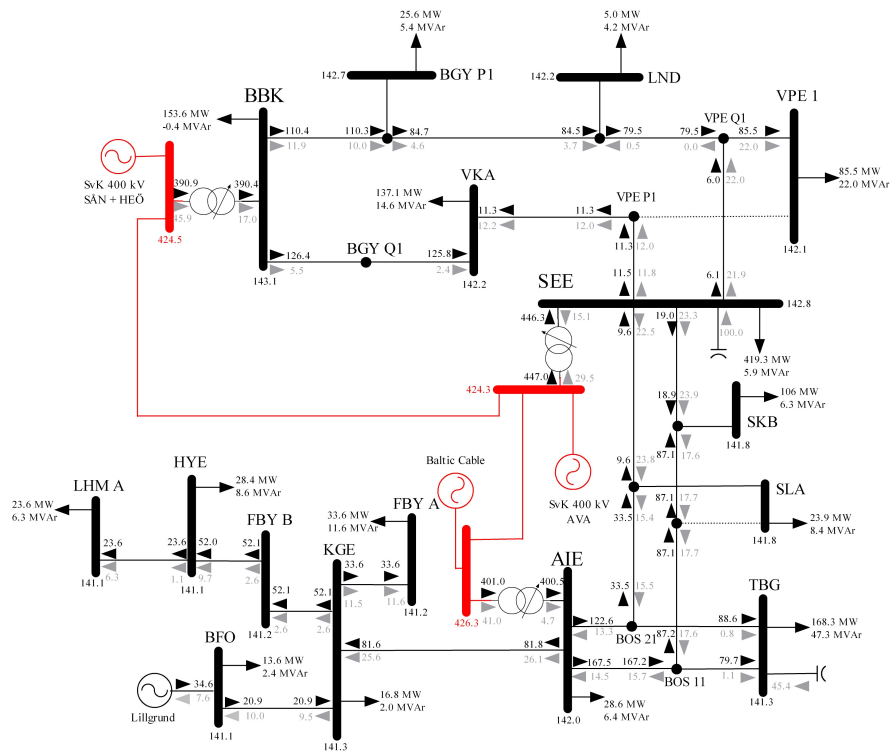
Figure 6.7 Load flow of the 130 kV grid model.

Table 6.2 Bus Voltages in the PSCAD model, the E.ON model and the differences.

	Bus Voltages [kV]			
Bus	E.ON. PSS/E model	The PSCAD model	Difference	Difference [%]
BBK 400kV	414.7	424.5	9.8	2.36
BBK 130kV	140.5	143.1	2.6	1.85
SEE 400kV	415.7	424.3	8.6	2.07
SEE 130kV	140.2	142.8	2.6	1.85
AIE 400kV	416.9	426.3	9.4	2.25
AIE 130kV	139.5	142	2.5	1.79
BFO	138.6	141.1	2.5	1.80
KGE	138.9	141.4	2.4	1.73

6.2 Fault Response

Measuring data was provided by E.ON for two faults. The first fault occurred on the 5th of January 2008 and was line to line fault near the BBK station. From this occasion, transient fault recorder (TFR) data was received from the SEE substation. Due to a lack

33

of grid components such as the Öresund power plant (Öresundsverket) which connects to the SEE substation, the only usable data were the voltage profiles on this bus. The second fault occurred on the 22nd of June 2008 during a lightning storm and was a single line to ground fault close to the BFO substation. Between these fault occasions, additional transient fault recorders had been installed in the BFO and KGE substations and it was therefore possible to use measuring data from those substations as well for the second fault. All transient fault recorders have 1 kHz sampling frequency.

The optimal fault response of the model was obtained by tuning of the fault impedance because it remains an unknown factor that greatly affects the fault response. The tuning was done based on the following factors

1. voltage/current profiles

2. amplitude

where the profiles were considered to be most important.

6.2.1   Fault Settings

Impedances with 70° angle were tried, but the occurred faults could not be reconstructed in that way. All fault impedances were therefore chosen purely resistive. The distance between the fault and the monitoring location affects the impedance and therefore the currents and voltages registered. Because this factor also is unknown, all faults were applied directly at the BBK and BFO buses.

6.2.2   Grid Configuration

Other factors affect the fault response, such as the grid configuration and load flow at the fault occasion. In this model, the configuration obtained by E.ON in the single-line diagram was used for all simulations and it is not known whether or not that was the correct configuration during the faults used for verification.

6.2.3   Barsebäck Line to Line Fault

The measured and simulated phase voltages from the SEE substation during the BBK fault are presented in Figure 6.8. It clearly appears that the fault is a line to line fault because of the obvious dip on two phases.

The figure clearly illustrates that the simulated result is close to the measured. As observed, high frequency characteristics from the grid appear in the simulation, although the amplitudes differ slightly. The amplitude of the simulated 50 Hz signal during the fault is approximately 30 % higher than the measured signal. The simulated graph also supports the assumption regarding the fault type.
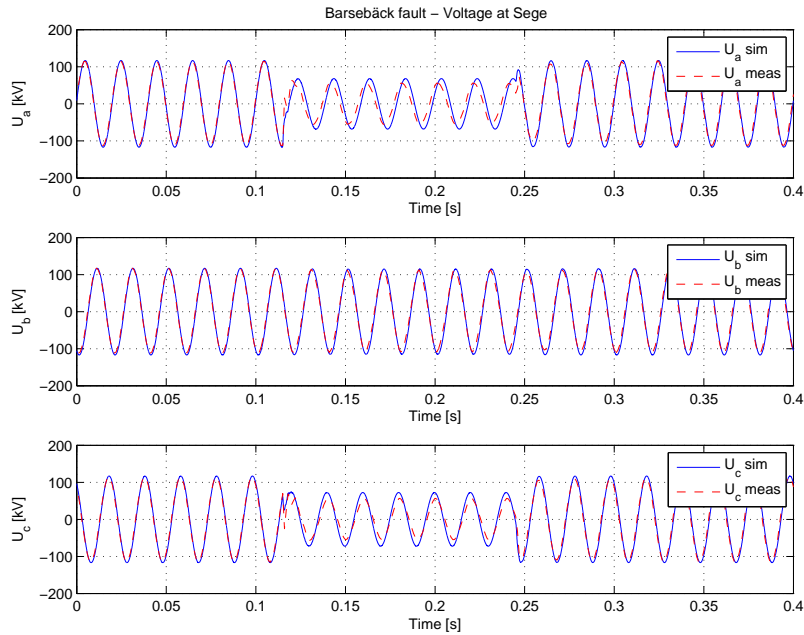
Figure 6.8 The fault response at SEE from the BBK fault, phase voltages.

6.2.4   Bunkeflo Line to Ground Fault

The measured and simulated voltages and currents from the BFO substation during the fault are presented in Figures 6.9 and 6.10 respectively. The current reference is such that the current is negative when power flows from Lillgrund into the substation.

Phase a is considered to be the most relevant phase to observe because the fault is applied there. Both the current and voltage amplitudes of the simulated 50 Hz signal during the steady-state part of the fault are almost identical with the measured signal. This is not the case on the other phases, where the deviation is notable but seen as less important because of the lower amplitudes. During the first half-period after the fault has been applied, a clear amplitude deviation is noted on all three phases.

Figures 6.11, 6.12 and show the voltage at the KGE substation along with the current between the KGE and AIE substations. Both the current and voltage profiles correspond well to each other during the fault, but the current differs before and after the fault. This difference corresponds to a difference in power flow, between KGE and AIE between the measurement and simulation. The voltage amplitude at KGE substation during the fault is around 42 % higher in the simulation than in reality, and the current is around 30 % lower. The graph also supports the assumption regarding the fault type.
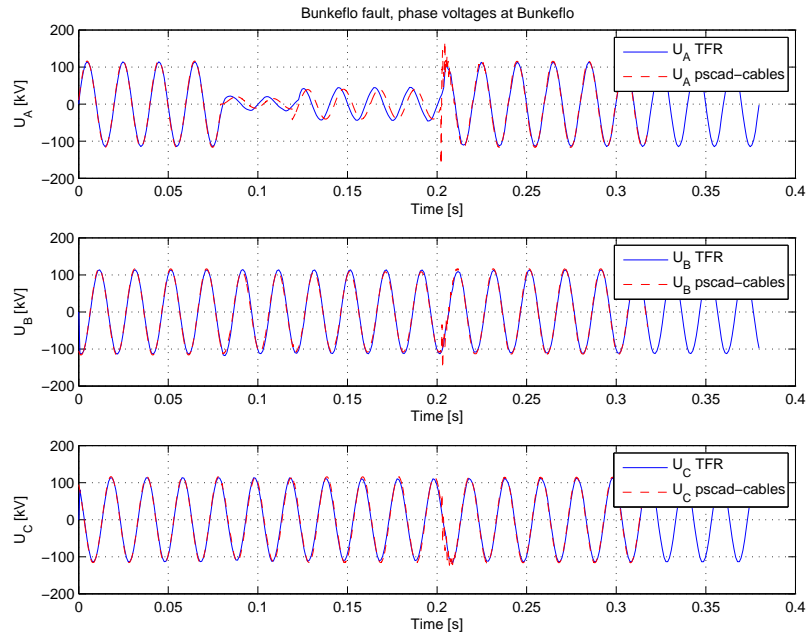
Figure 6.9 Measured and simulated voltages at the BFO substation during the fault.
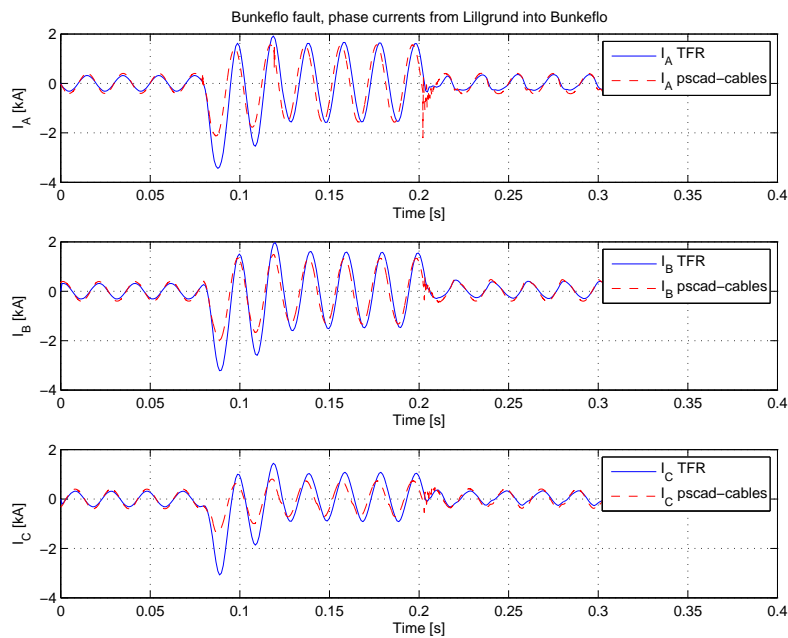

Figure 6.10 The current from the BFO substation into Lillgrund during the fault.
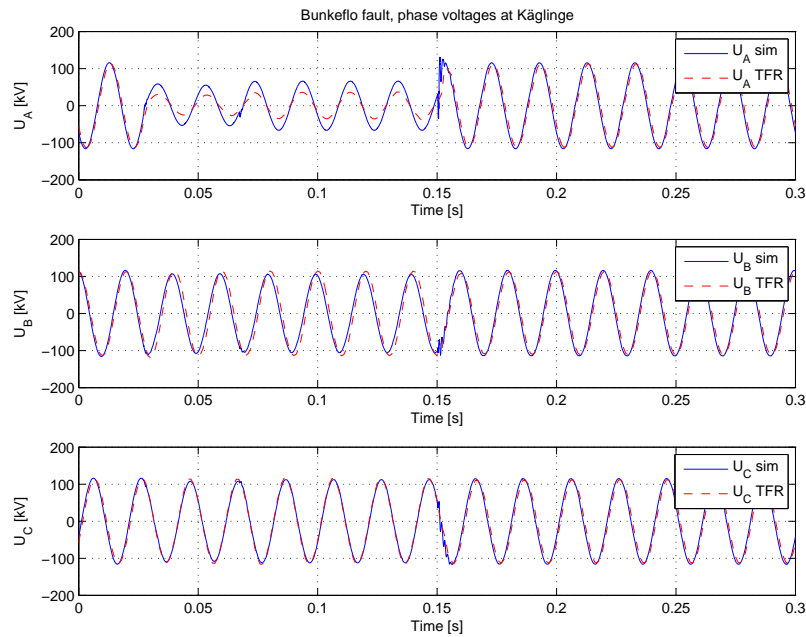
Figure 6.11 The voltages at the KGE substation during the fault.
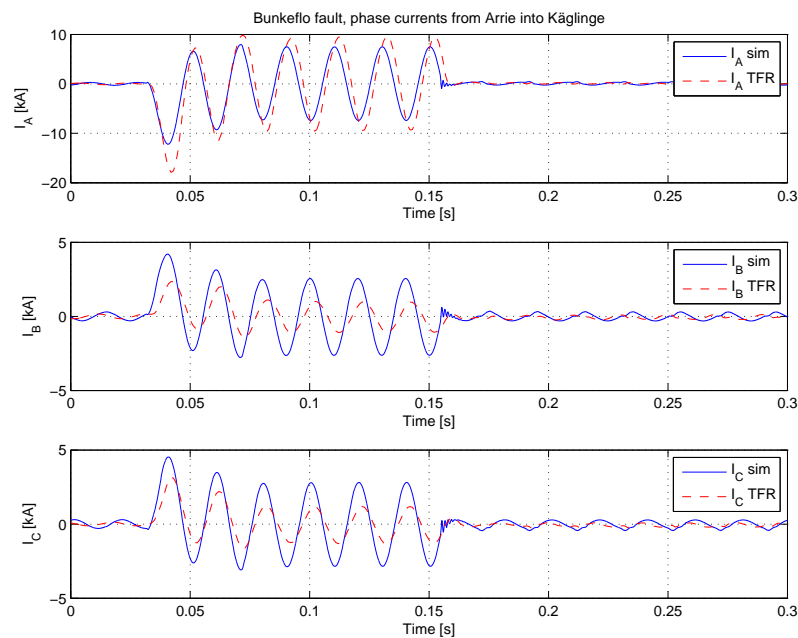
Figure 6.12 The currents coming from AIE into the KGE substation during the fault.
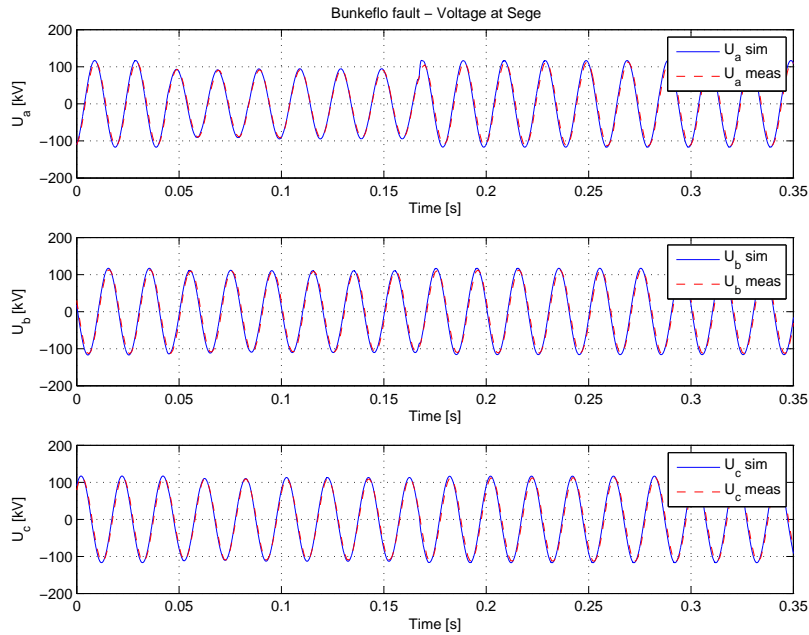
Figure 6.13 The voltages at the SEE substation during
the single line-to-ground fault.

As observed in Figure 6.13, the simulated and measured voltages correspond well to each
other at the SEE substation.

6.3   Lillgrund Wind Farm

Due to the fact that there is no information on voltages and currents within the wind
farm, no verification can be done for the values inside it. The only known fact is that no
turbine tripped during any of the simulated faults.

6.4   Verification Conclusions

All voltages and currents had similar profiles, which was set to be the most important
factor. High frequency components were seen in some simulation cases but not in the
measured data, possibly due to the limited sampling frequency of the transient recorders.
Lack of information concerning the grid configuration at the time of the faults may con-
tribute to deviations in both current and voltage amplitudes during faults.

Load flow differences were seen when comparing Figures 6.7 and 5.6. To get exactly
the same load flow was seen as an impossible task since there are so many factors in-
volved affecting the result. The load flow in the given single-line diagram was obtained
from simulations, introducing an error from the beginning. The deviations in the load
flows and bus voltages of the model are kept well within the limits.

Since no information was found about the correct load flow, grid configuration, exact

fault location or fault impedance on the fault occasions, a loss in accuracy will follow. The loss in accuracy due to these different contributions is difficult to estimate. The load flow is a result of the various impedances in the grid and by observing the load flows during steady-state, it is concluded that the grid is very well modeled compared to E.ONs PSS/E model because of the small load flow and voltage deviations.

There are notable differences in the transient behaviour despite the accurate load flow results. The assumption that the faults were purely resistive and applied directly at buses, because they are unknown as described in 6.2, is believed to contribute to these deviations. As stated in section 6.2.4, a high amplitude deviation is observed during the first half period. This is believed to have four possible causes:

- differences in the zero-sequence impedance between the model and reality.

- differences in the X/R ratio between the model and reality.

- the transient reactance and resistances of the wind turbine induction generators.

- the fault is simulated as a pure short circuit, while it might have been caused by a lightning strike, which means additional energy injection that is not taken into account in the simulation.

The large transformer Z_0 variation, as stated in section 5.3, means that the current may vary within a wide range as well during unbalanced faults to earth. Since the transformer tap setting at the time of the fault is unknown [44], it is not possible to know whether or not the Z_0 is correct in this model either. Another argument against the Z_0 being a problem, is that the current amplitudes during the steady-state are very similar according to Figure 6.10. According to [4], the X/R ratio affects the initial current amplitude and phase shift. The wind turbine models lack induction generators, meaning that the short circuit characteristics may differ from those of the current sources. On the other hand, it was decided that the controllable current sources represent the full power converter in an adequate way due to its switching frequency.

7 Simulations

To see how different kinds of faults, applied at different locations in the connecting grid would affect the voltage magnitude at the turbines as well as at the 138/33 kV transformer, the busses at SEE, AIE, KGE and BFO substations were chosen as fault locations.

Since a single line to ground fault (SLG) and a line to line fault (LL) have been used for verifications of the grid model, these types of faults have been simulated to represent commonly occurring unbalanced faults in the grid. Different types of balanced voltage dips due to faults or common events in the grid have also been simulated, which are presented in the end of this section.

A different number of connected radials as well as the amount of generated power when a fault occurs, may give differences in the results. For that reason a number of configurations were selected, with different numbers of connected radials along with one case with a different amount of generated power. All cases of interest are listed below

- All five radials operating at maximum power output.

- All five radials are on idle operation.

- Radial 1,2 and 5 connected and operating at maximum power output.

- Radial 1 connected and operating at maximum power output.

Radial 1 includes monitoring points at turbines E-02, H-02 and H-04. Radial 2 includes monitoring points at turbines D-01, E-04 and F-06. Radial 5 includes monitoring points at turbines A-01 and B-08. The monitoring points at the turbines are located at the high voltage side of the 33/0.69 kV transformer. Radials 3 and 4 are simulated using PI-models to reduce the simulation time, but also since no monitoring points are located here. For all cases, monitoring points are located at the low and high voltage side of the 138/33 kV transformer. The selected monitoring locations and their radials are shown in Figure 7.1, where the phase to ground voltage U_{ph-gnd} for all three phases is measured.

From these measurements, the maximum peak value $|\hat{U}|_{max}$ and the minimum peak value $|\hat{U}|_{min}$ in per unit (pu) were determined. The crest voltages $|\hat{U}|_{ph-gnd}$ of the main 138/33 kV transformer ratings, were selected as base voltages U_{base}.

The performed simulations are presented in separate tables for each case, where the extreme values of under voltage and over voltage are presented. The maximum magnitude difference between two phases for each fault type are presented for future investigation of differential protection. From each case, the fault response generating the minimum voltage and the maximum voltage will be presented in the time domain. Some results in the tables are rounded off, for a more clearer presentation. Each table consist of a column with appendix references numbers to all plots in the time domain for all simulated cases. These plots are only available in the extended version of this report, which is handed out to Vattenfall Power Consultant for further analysis of the results.
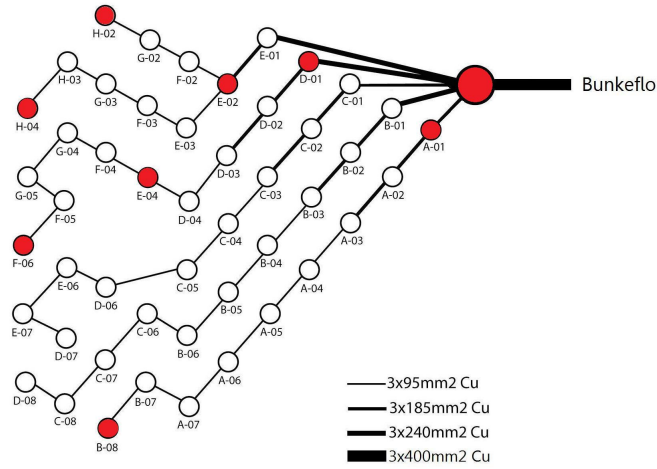
Figure 7.1 The selected monitoring points at Lillgrund.

The faults have been applied at the crest voltage of phase a $(\hat{U}_a)$ in all cases, except for one case of a single line to ground fault, where the fault was applied at the zero crossing $|U_a| = 0$. This was done to see if it would affect the voltage magnitude in any way. All applied faults in the 130 kV grid were simulated during 150 ms due to the assumed fast fault clearing time in this kind of grid. At all fault simulations, it was assumed that there would be some remaining voltage at the fault location. The amount of remaining voltage in each case was assumed to characterize a real fault.

Simulations of single line to ground faults were performed using a fault impedance of 0.5 Ω, which would give 0.05 pu - 0.1 pu remaining voltage at the fault location during the fault. It was assumed that a common event such as a lightning strike, approximately would give this amount of remaining voltage.

Line to line fault simulations were performed using a fault impedance of 1.65 Ω between phase a and phase b. This fault impedance was used for the recreation of the line to line fault close to Barsebäck when verifying the grid model.

Three different cases regarding balanced voltage dips have been simulated, each representing different events. One case (3ph) represents a severe voltage dip due to a three phase to ground short circuit fault. A fault impedance of 0.5 Ω [38] were used to represent a non-bolted fault, which would give approximately 0.05 pu - 0.1 pu remaining voltage at the fault location during this fault. The second case (3ph 90 %) represent a switching event in the grid e.g. starting of a large motor. The remaining voltage at the affected bus was assumed to be 90 % [38] of the pre-fault voltage, which was achieved by using a fault impedance between 18 - 40 Ω at the different fault busses. Finally, the short term voltage variation in Figure 3.2, given by the grid codes (SvK) in section 3.2 were applied at the SEE substation.

7.1   Turbines at Maximum Power, All Radials Connected

In this case, the turbines are operating at maximum power output and all five radials are connected. The results due to different types of faults applied at different locations in the connecting grid 130 kV grid, are seen in Table 7.1.

Table 7.1 Results- Turbines at maximum power output and all radials connected.

Results from simulations of U_{ph-gnd} when turbines are operating at maximum power output and all radials connected											
Fault type	Applied Location		$U_{base} = 26.94kV$				$U_{base} = 112.7kV$				
			Wind turbine			TRF LV	E.ON grid, $|\hat{U}|_{min}$ [pu]				TRF HV
		App.	$|\hat{U}|_{min}$ [pu]	$\hat{U}_{diff}$ [%]	$|\hat{U}|_{max}$ [pu]	$|\hat{U}|_{max}$ [pu]	BFO	KGE	AIE	SEE	$|\hat{U}|_{max}$ [pu]
SLG at $\hat{U}$	BFO	D.1	E-02: 0.529	F-06: 49.16	F-06: 1.22	1.20	0.052	0.468	0.68	0.806	1.14
	KGE	D.6	E-02: 0.498	F-06: 51.64	F-06: 1.14	1.11	0.15	0.082	0.432	0.659	1.07
	AIE	D.11	E-02: 0.52	F-06: 49.28	F-06: 1.06	1.05	0.227	0.172	0.12	0.452	1.04
	SEE	D.16	A-01: 0.597	E-02: 41.42	F-06: 1.07	1.05	0.434	0.41	0.377	0.135	1.04
SLG at $|U|_{min}$	BFO	D.2	E-02: 0.527	F-06: 49.39	F-06: 1.21	1.19	0.052	0.467	0.678	0.805	1.11
	KGE	D.7	E-02: 0.494	F-06: 52.15	F-06: 1.1	1.09	0.146	0.082	0.43	0.657	1.06
	AIE	D.12	E-02: 0.518	F-06: 49.58	F-06: 1.06	1.04	0.22	0.17	0.119	0.451	1.04
	SEE	D.17	A-01: 0.599	E-02: 41.24	F-06: 1.05	1.04	0.43	0.408	0.376	0.134	1.04
LL	BFO	D.3	A-01: 0.131	A-01: 85.71	F-06: 1.36	1.31	0.453	0.588	0.715	0.799	1.16
	KGE	D.8	A-01: 0.152	A-01: 83.18	F-06: 1.59	1.50	0.446	0.42	0.582	0.708	1.09
	AIE	D.13	A-01: 0.111	A-01: 87.46	F-06: 1.45	1.41	0.428	0.404	0.391	0.577	1.06
	SEE	D.18	A-01: 0.308	A-01: 66.60	F-06: 1.12	1.09	0.538	0.523	0.516	0.383	1.04
3ph	BFO	D.4	A-01: 0.126	D-01: 4.643	F-06: 1.37	1.33	0.01	0.348	0.576	0.726	1.11
	KGE	D.9	A-01: 0.107	A-01: 6.51	F-06: 1.62	1.55	0.041	0.071	0.36	0.576	1.05
	AIE	D.14	A-01: 0.103	B-08: 10.30	F-06: 1.42	1.37	0.059	0.086	0.104	0.361	1.04
	SEE	D.19	A-01: 0.305	A-01: 2.04	F-06: 1.05	1.04	0.264	0.261	0.262	0.119	1.04
3ph 90 %	BFO	D.5	A-01: 0.918	F-06: 0.88	F-06: 1.22	1.17	0.934	0.958	0.977	0.994	1.07
	KGE	D.10	A-01: 0.897	A-01: 0.84	F-06: 1.58	1.53	0.917	0.919	0.946	0.968	1.07
	AIE	D.15	A-01: 0.896	E-04: 0.84	F-06: 1.26	1.22	0.914	0.918	0.924	0.947	1.05
SvK	SEE	D.20	A-01: 0.226	A-01: 2.18	F-06: 1.05	1.04	0.094	0.065	0.051	0.066	1.04

A minimum voltage of 0.103 pu (2.77 kV) is to be found at turbine A-01 due to a three phase to ground fault in AIE, which is shown in Figure 7.2.

A maximum voltage of 1.62 pu (43.64 kV) is to be found at turbine F-06 due to a three phase to ground fault at KGE in the beginning of the applied fault, as seen in Figure 7.3.

A maximum difference of 87.46 % in amplitude is found at turbine A-01, during a line to line fault at AIE.

At the platform, the low voltage side of the main transformer will experience a maximum voltage of 1.55 pu (41.76 kV) when there is a three phase to ground fault at KGE.

The minimum voltage registered at BFO due to the SvK voltage profile applied at SEE, is 0.094 pu (10.6 kV). At the turbine A-01 the minimum voltage due to this fault is 0.226 pu (6.09 kV).
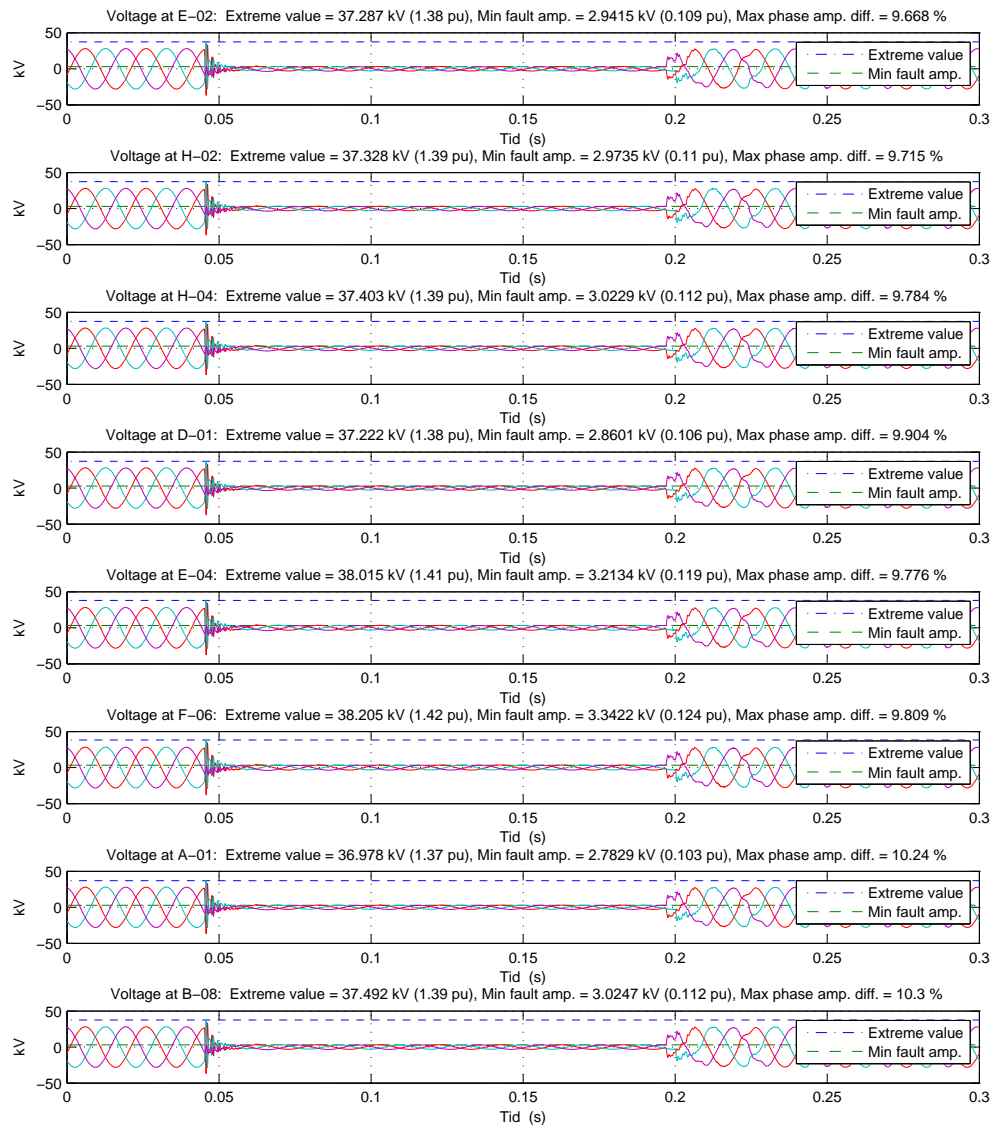
Figure 7.2 Turbine voltages due to a three phase to ground fault in AIE when all five radials operate at maximum.
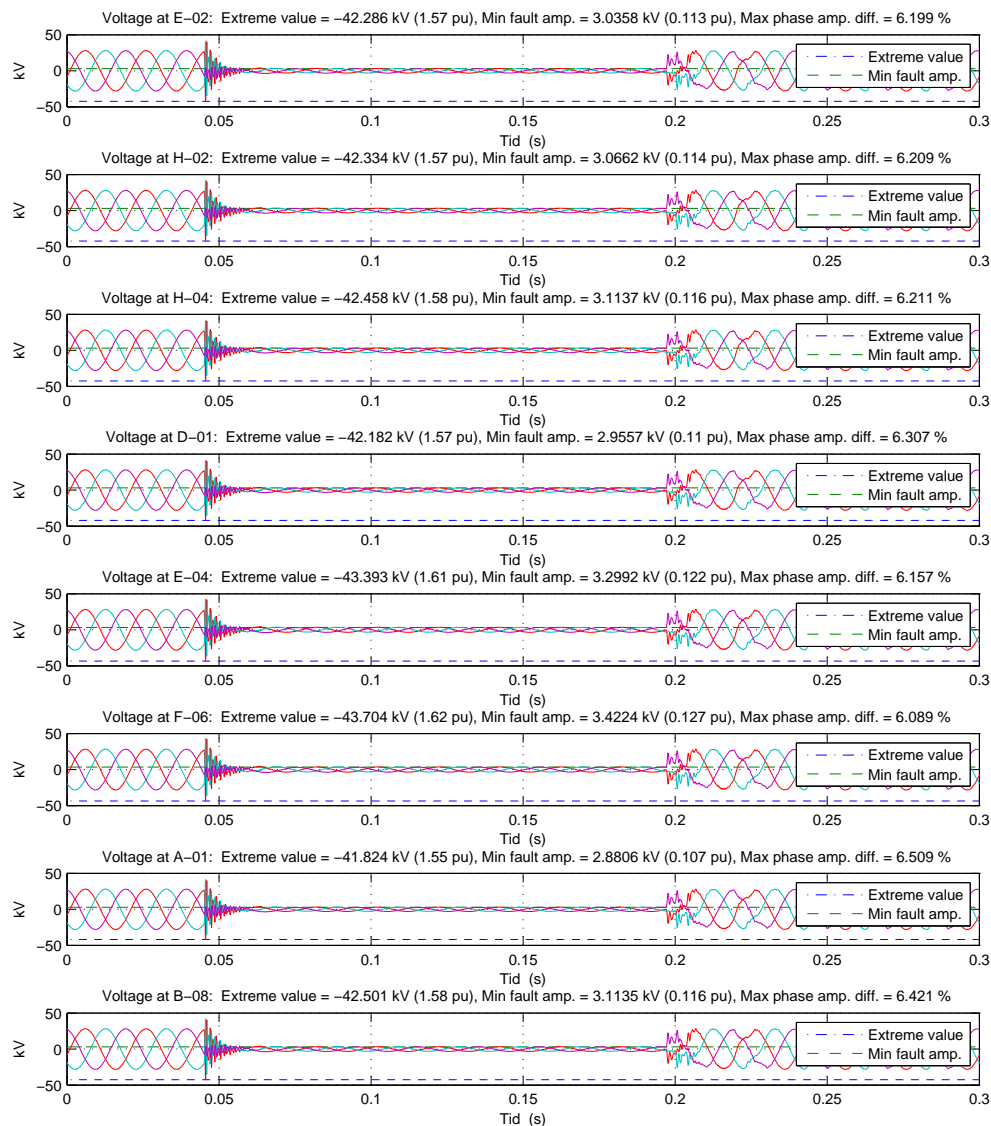
Figure 7.3 Turbine voltages due to a three phase to ground fault in KGE when all five radials operate at maximum.

7.2   Turbines on Idle Operation, All Radials Connected

When Lillgrund is not generating any power, it will only consume a certain amount of power. The results due to faults in the connecting grid, when all five radials are connected and on the turbines are on idle operation, are seen in Table 7.2.

Table 7.2 Results- Turbines on idle operation and all radials connected.

Results from simulations of U_{ph-gnd} when turbines are on idle operation and all radials connected											
Fault type	Applied Location		$U_{base} = 26.94kV$				$U_{base} = 112.7kV$				
			Wind turbine			TRF LV	E.ON grid, $|\hat{U}|_{min}$ [pu]				TRF HV
		App.	$|\hat{U}|_{min}$ [pu]	$\hat{U}_{diff}$ [%]	$|\hat{U}|_{max}$ [pu]	$|\hat{U}|_{max}$ [pu]	BFO	KGE	AIE	SEE	$|\hat{U}|_{max}$ [pu]
SLG at $\hat{U}$	BFO	E.1	E-02: 0.535	All: 47.87	F-06: 1.18	1.17	0.051	0.464	0.678	0.804	1.13
	KGE	E.6	E-02: 0.532	E-01: 47.72	F-06: 1.11	1.10	0.15	0.081	0.43	0.657	1.07
	AIE	E.11	H-04: 0.519	H-04: 48.82	F-06: 1.04	1.04	0.227	0.176	0.119	0.449	1.03
	SEE	E.16	E-02: 0.62	F-06: 38.55	F-06: 1.05	1.05	0.424	0.405	0.374	0.134	1.03
SLG at $|U|_{min}$	BFO	E.2	E-02: 0.538	E-02: 47.66	F-06: 1.16	1.17	0.051	0.463	0.676	0.803	1.10
	KGE	E.7	All: 0.541	E-02: 46.97	F-06: 1.1	1.10	0.152	0.081	0.427	0.655	1.05
	AIE	E.12	E-02: 0.53	E-02: 47.72	F-06: 1.04	1.04	0.224	0.176	0.118	0.448	1.03
	SEE	E.17	E-02: 0.625	E-02: 38.11	F-06: 1.03	1.03	0.422	0.403	0.373	0.133	1.03
LL	BFO	E.3	All: 0.084	All: 90.85	F-06: 1.36	1.33	0.451	0.599	0.701	0.789	1.17
	KGE	E.8	E-02: 0.123	E-02: 86.73	F-06: 1.56	1.47	0.418	0.418	0.585	0.697	1.07
	AIE	E.13	E-02: 0.175	E-02: 81.57	F-06: 1.31	1.29	0.388	0.387	0.387	0.578	1.05
	SEE	E.18	H-02: 0.302	H-02: 67.38	F-06: 1.06	1.05	0.508	0.507	0.508	0.38	1.03
3ph	BFO	E.4	F-06: 0.045	F-06: 16.26	F-06: 1.06	1.05	0.045	0.36	0.582	0.728	1.05
	KGE	E.9	B-08: 0.068	B-08: 13.38	F-06: 1.65	1.56	0.07	0.07	0.357	0.575	1.03
	AIE	E.14	B-08: 0.1	B-08: 11.38	F-06: 1.4	1.35	0.102	0.102	0.103	0.358	1.03
	SEE	E.19	B-08: 0.256	B-08: 3.108	F-06: 1.03	1.03	0.258	0.259	0.26	0.118	1.03
3ph 90 %	BFO	E.5	All: 0.926	A-01: 1.342	F-06: 1.16	1.12	0.921	0.944	0.965	0.984	1.06
	KGE	E.10	E-02: 0.92	F-06: 0.879	F-06: 1.53	1.49	0.92	0.919	0.943	0.965	1.06
	AIE	E.15	H-04: 0.924	F-06: 0.68	F-06: 1.21	1.18	0.925	0.924	0.928	0.949	1.05
SvK	SEE	E.20	A-01: 0.036	B-08: 12.55	A-01: 1.03	1.03	0.038	0.038	0.039	0.063	1.03

A minimum voltage of 0.045 pu (1.21 kV) is to be found at turbine F-06 due to a three phase to ground fault in BFO, which is shown in Figure 7.4.

A maximum voltage of 1.65 pu (44.45 kV) is to be found at turbine F-06 due to a three phase to ground fault in KGE, as seen in Figure 7.5.

A maximum difference of 90.85 % in amplitude between two phases is found at all turbines, during a line to line fault at BFO.

At the platform, the low voltage side of the main transformer will experience a maximum voltage of 1.56 pu (42.03 kV) when there is a three phase to ground fault at KGE.

The minimum voltage registered at BFO due to the SvK voltage profile applied at SEE, is 0.038 pu (4.28 kV). At the turbine A-01 the minimum voltage due to this fault is 0.036 pu (0.97 kV).
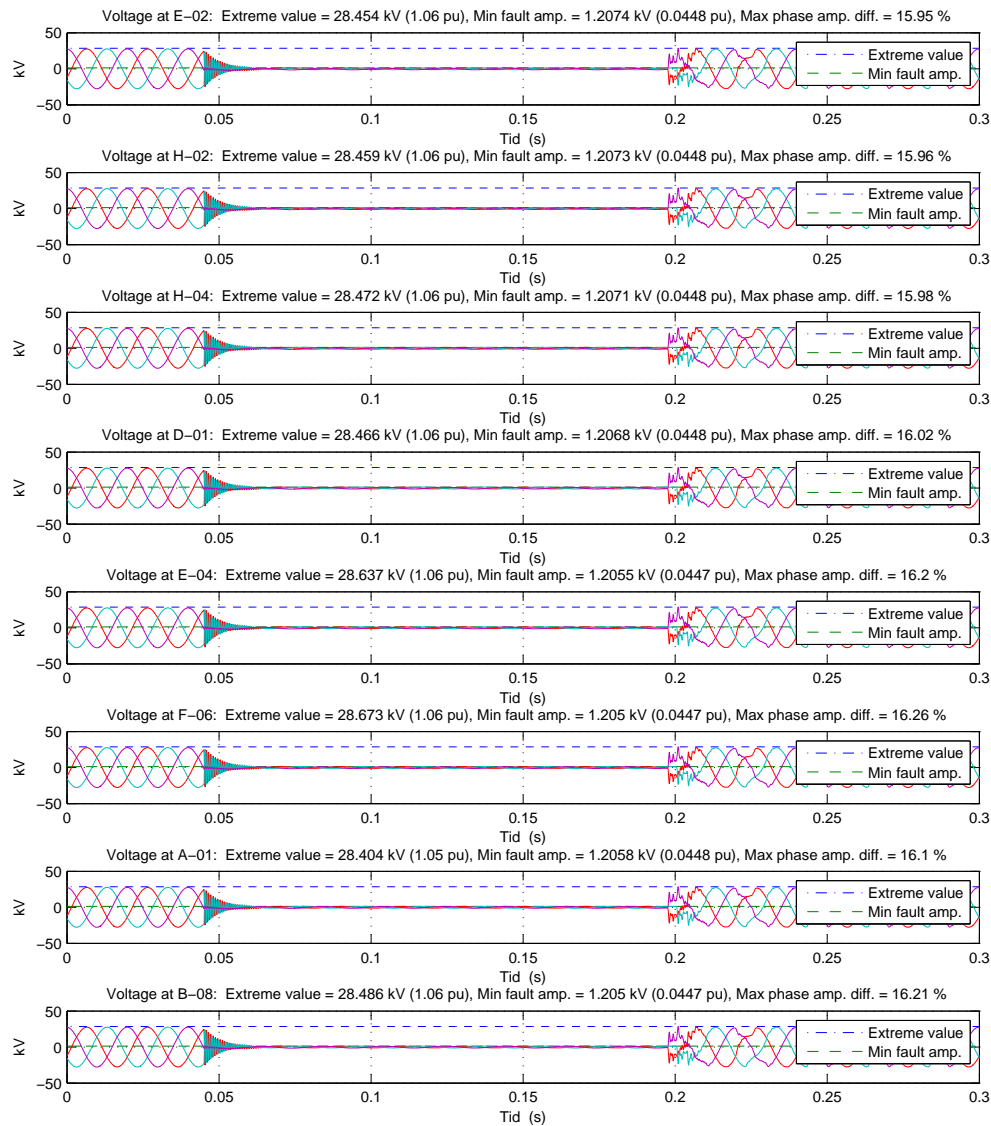
Figure 7.4 Turbine voltages due to a three phase to ground fault in BFO when all turbines are on idle operation.
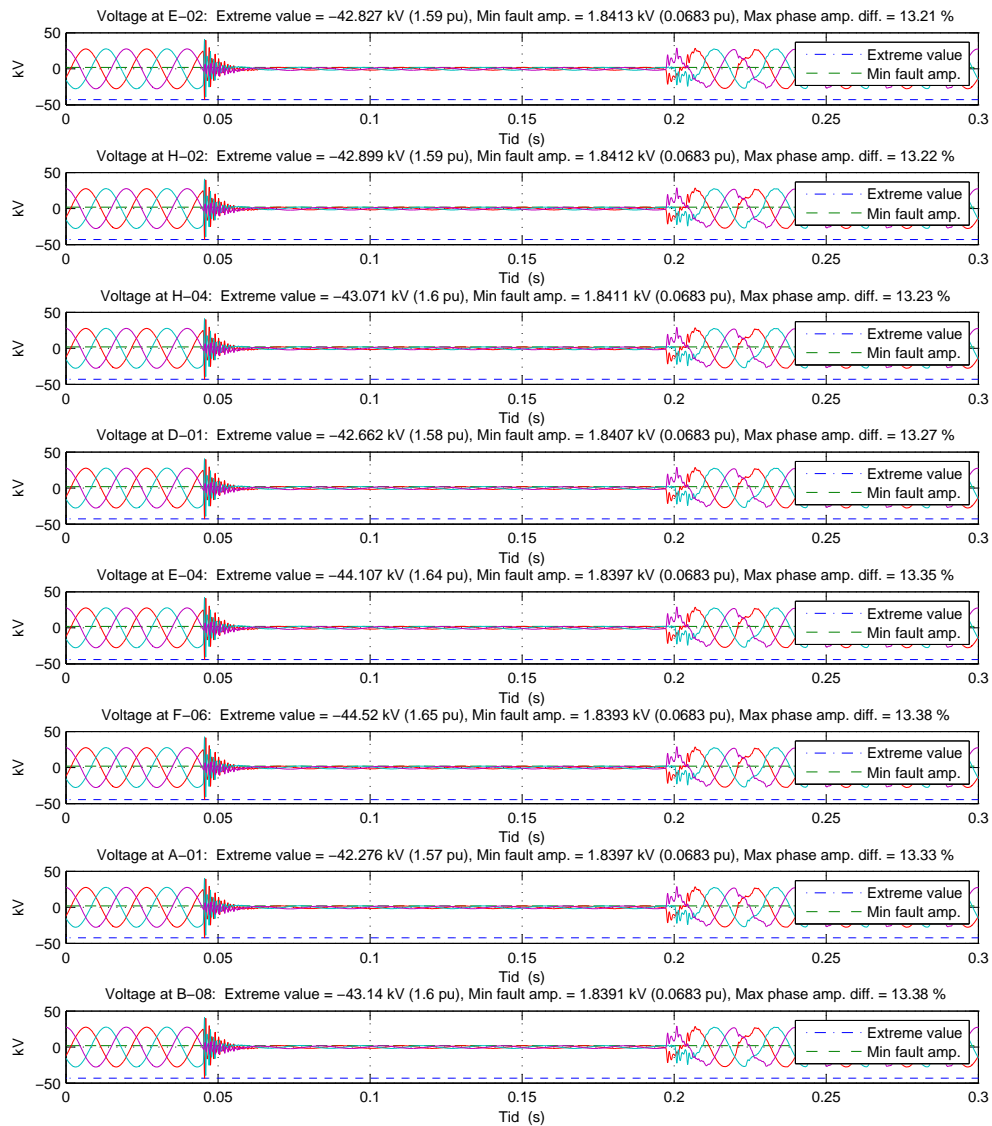
Figure 7.5 Turbine voltages due to a three phase to ground fault in KGE when all turbines are on idle operation.

7.3 Turbines at Maximum Output, Radials 1,2 and 5 Connected

In this case, the turbines are generating maximum power output and radial 1, 2 and 5 are connected. The results due to different types of faults in the connecting grid, are seen in Table 7.3.

Table 7.3 Results- Turbines at maximum power output and radial 1,2 and 5 connected.

Results from simulations of U_{ph-gnd} when turbines are operating at maximum power output and radials 1, 2 and 5 are connected											
Fault type	Applied Location		$U_{base} = 26.94kV$				$U_{base} = 112.7kV$				
			Wind turbines			TRF LV	E.ON grid, $|\hat{U}|_{min}$ [pu]				TRF HV
		App.	$|\hat{U}|_{min}$ [pu]	$\hat{U}_{diff}$ [%]	$|\hat{U}|_{max}$ [pu]	$|\hat{U}|_{max}$ [pu]	BFO	KGE	AIE	SEE	$|\hat{U}|_{max}$[pu]
SLG at $\hat{U}$	BFO	F.1	E-02: 0.551	F-06: 46.77	F-06: 1.21	1.18	0.052	0.466	0.679	0.805	1.16
	KGE	F.6	E-02: 0.526	F-06: 48.73	F-06: 1.14	1.12	0.149	0.082	0.431	0.658	1.09
	AIE	F.11	E-02: 0.549	F-06: 46.21	F-06: 1.07	1.06	0.226	0.173	0.119	0.45	1.03
	SEE	F.16	A-01: 0.612	E-02: 39.50	F-06: 1.08	1.06	0.429	0.408	0.376	0.134	1.03
SLG at $|U|_{min}$	BFO	F.2	E-02: 0.548	F-06: 47.03	F-06: 1.19	1.17	0.051	0.465	0.678	0.804	1.14
	KGE	F.7	E-02: 0.523	F-06: 49.09	F-06: 1.13	1.12	0.146	0.082	0.429	0.656	1.08
	AIE	F.12	E-02: 0.546	F-06: 46.45	F-06: 1.05	1.04	0.219	0.172	0.118	0.45	1.03
	SEE	F.17	A-01: 0.615	E-02: 39.28	F-06: 1.05	1.03	0.426	0.406	0.375	0.133	1.03
LL	BFO	F.3	A-01: 0.092	A-01: 89.60	F-06: 1.25	1.21	0.453	0.593	0.71	0.795	1.14
	KGE	F.8	A-01: 0.080	A-01: 90.93	F-06: 1.56	1.46	0.435	0.419	0.584	0.704	1.08
	AIE	F.13	D-01: 0.106	D-01: 88.25	F-06: 1.32	1.28	0.413	0.397	0.389	0.578	1.06
	SEE	F.18	A-01: 0.297	A-01: 66.64	F-06: 1.08	1.06	0.514	0.511	0.51	0.381	1.04
3ph	BFO	F.4	A-01: 0.041	A-01: 15.47	F-06: 1.09	1.07	0.046	0.362	0.583	0.729	1.07
	KGE	F.9	A-01: 0.042	A-01: 23.95	F-06: 1.59	1.51	0.052	0.07	0.359	0.576	1.04
	AIE	F.14	A-01: 0.041	A-01: 28.86	F-06: 1.23	1.18	0.074	0.092	0.103	0.36	1.03
	SEE	F.19	A-01: 0.267	A-01: 2.473	F-06: 1.04	1.03	0.26	0.26	0.261	0.119	1.03
3ph 90 %	BFO	F.5	A-01: 0.916	E-02: 1.153	F-06: 1.28	1.21	0.928	0.952	0.973	0.991	1.07
	KGE	F.10	A-01: 0.906	F-06: 1.155	F-06: 1.33	1.29	0.922	0.922	0.947	0.969	1.08
	AIE	F.15	A-01: 0.906	F-06: 1.024	F-06: 1.10	1.07	0.92	0.922	0.927	0.949	1.05
SvK	SEE	F.20	A-01: 0.144	A-01: 2.18	F-06: 1.04	1.03	0.067	0.052	0.045	0.064	1.03

A minimum voltage of 0.041 pu (1.10 kV) is to be found at turbine A-01 due to a three phase to ground fault in in BFO, which is shown in Figure 7.6.

A maximum voltage of 1.59 pu (42.83 kV) is to be found at turbine F-06 due to a three phase to ground fault in KGE, as seen in Figure 7.7.

A maximum difference of 90.93 % in amplitude of two phases is found at turbine A-01, during a line to line fault at KGE.

At the platform, the low voltage side of the main transformer will experience a maximum voltage of 1.51 pu (40.68 kV) when there is a three phase to ground fault at KGE.

The minimum voltage registered at BFO due to the SvK voltage profile applied at SEE, is 0.067 pu (7.55 kV). At the turbine A-01 the minimum voltage due to this fault is 0.144 pu (3.88 kV).
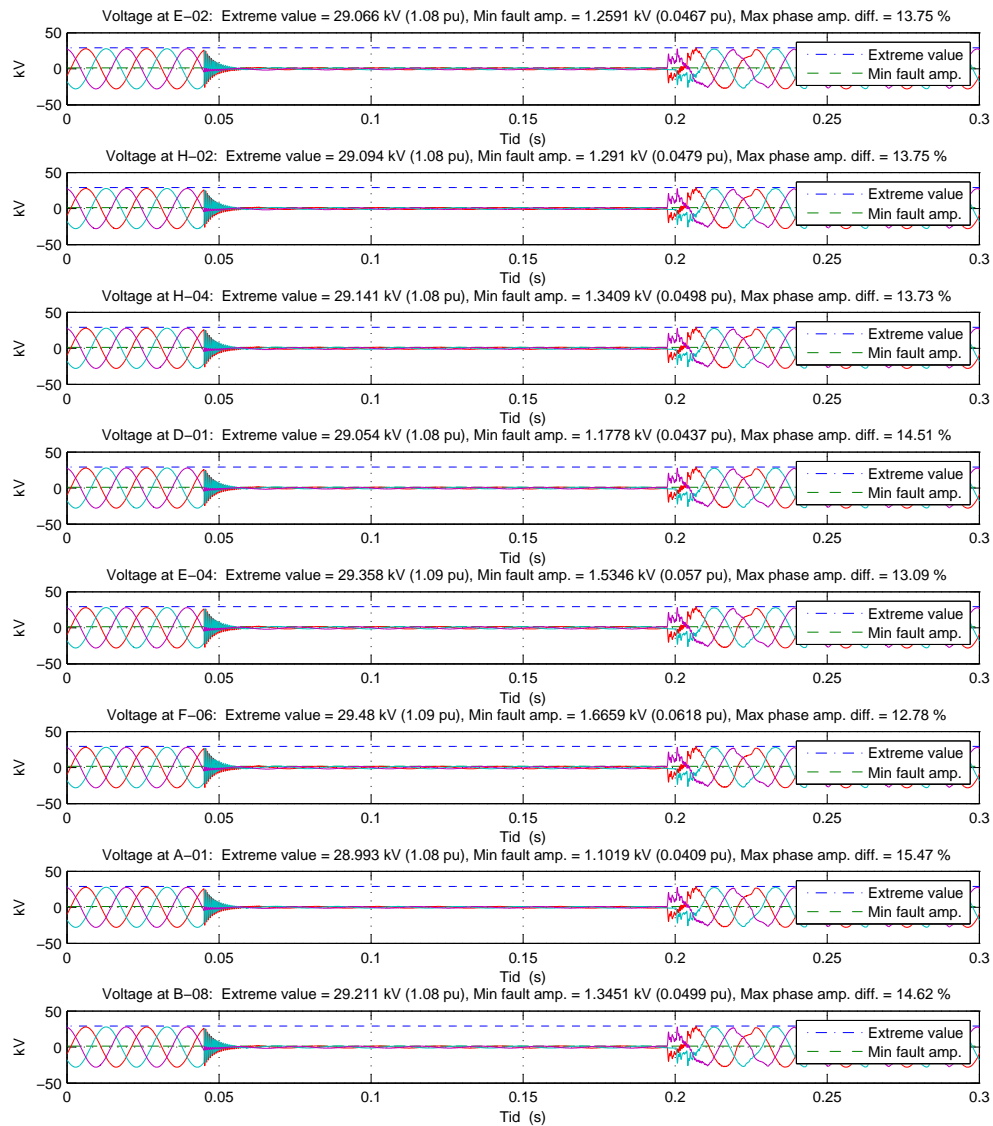
Figure 7.6 Turbine voltages due to a three phase to ground fault in BFO when radials 1, 2 and 5 are connected and the turbines operate at maximum.
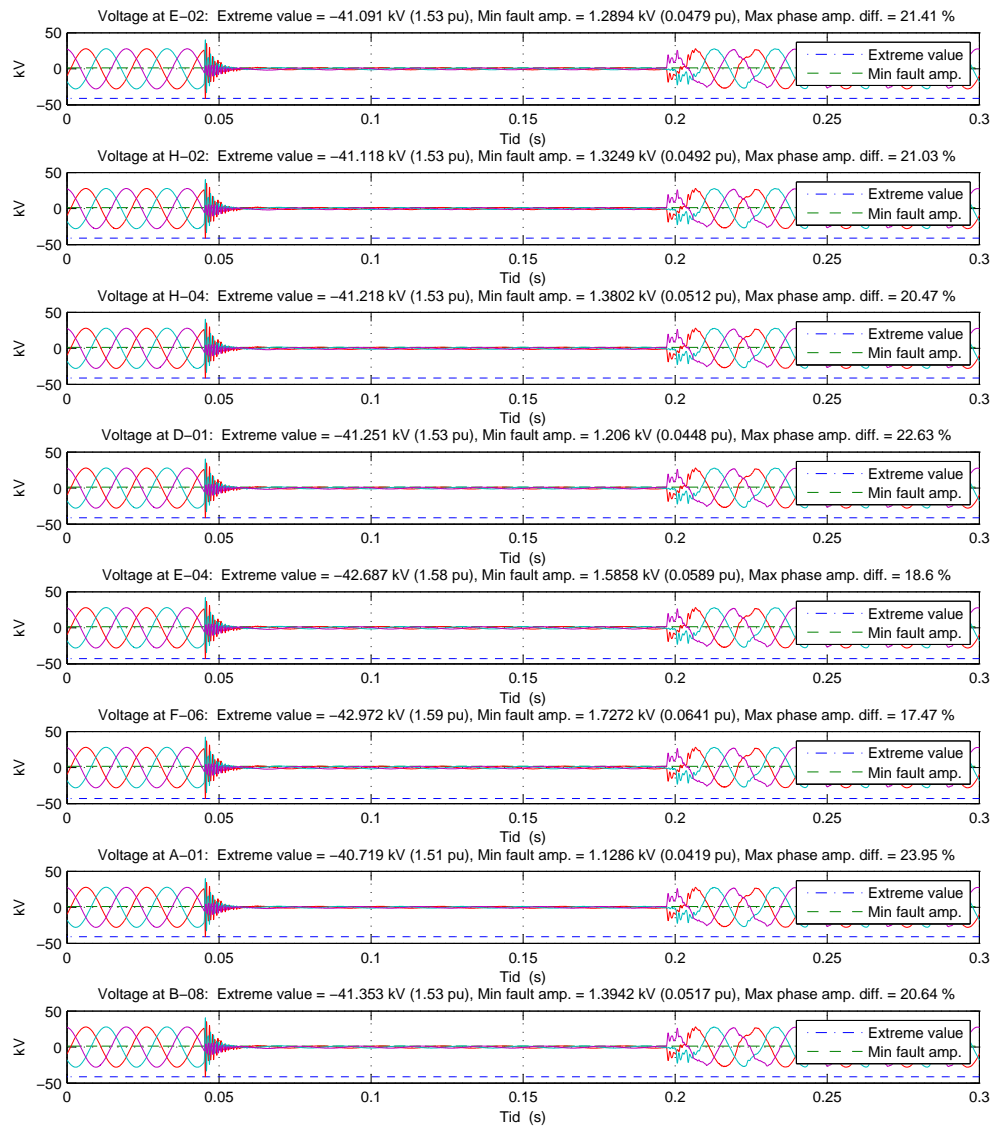
Figure 7.7 Turbine voltages due to a three phase to ground fault in KGE when radials 1, 2 and 5 are connected and the turbines operate at maximum.

7.4 Turbines at Maximum Power, Radial 1 Connected

In this case, the turbines are generating maximum output power and only radial 1 is connected. The results due to different types of faults in the connecting grid, are seen in Table 7.4.

Table 7.4 Results- Turbines at maximum power output and radial 1 connected.

Results from simulations of U_{ph-gnd} when turbines are operating at maximum power output and radial 1 is connected											
Fault type	Applied Location		$U_{base} = 26.94kV$				$U_{base} = 112.7kV$				
			Wind turbine			TRF LV	E.ON grid, $|\hat{U}|_{min}$ [pu]				TRF HV
		App.	$|\hat{U}|_{min}$ [pu]	$\hat{U}_{diff}$ [%]	$|\hat{U}|_{max}$ [pu]	$|\hat{U}|_{max}$ [pu]	BFO	KGE	AIE	SEE	$|\hat{U}|_{max}$ [pu]
SLG at $\hat{U}$	BFO	G.1	E-02: 0.565	E-02: 45.02	H-04: 1.17	1.16	0.051	0.465	0.678	0.804	1.15
	KGE	G.6	E-02: 0.577	E-02: 43.47	H-04: 1.14	1.13	0.152	0.081	0.43	0.658	1.09
	AIE	G.11	E-02: 0.563	E-02: 44.6	H-04: 1.09	1.08	0.229	0.175	0.119	0.449	1.03
	SEE	G.16	E-02: 0.652	E-02: 35.71	H-02: 1.08	1.07	0.426	0.405	0.375	0.134	1.03
SLG at $|U|_{min}$	BFO	G.2	E-02: 0.572	E-02: 44.52	H-04: 1.16	1.15	0.051	0.464	0.667	0.803	1.14
	KGE	G.7	E-02: 0.579	E-02: 43.26	H-04: 1.14	1.13	0.149	0.081	0.428	0.656	1.09
	AIE	G.12	E-02: 0.576	E-02: 43.21	H-04: 1.09	1.08	0.221	0.174	0.118	0.472	1.03
	SEE	G.17	E-02: 0.657	E-02: 35.04	H-04: 1.08	1.06	0.423	0.404	0.374	0.133	1.03
LL	BFO	G.3	H-02: 0.077	H-02: 91.48	H-04: 1.41	1.24	0.452	0.597	0.704	0.791	1.12
	KGE	G.8	E-02: 0.122	E-02: 86.67	H-04: 1.16	1.15	0.424	0.418	0.585	0.7	1.08
	AIE	G.13	E-02: 0.181	E-02: 80.59	H-04: 1.11	1.10	0.396	0.39	0.388	0.578	1.05
	SEE	G.18	E-02: 0.298	E-02: 67.53	H-04: 1.08	1.07	0.514	0.511	0.510	0.381	1.04
3ph	BFO	G.4	E-02: 0.014	E-02: 41.8	H-04: 1.52	1.34	0.045	0.361	0.582	0.729	1.08
	KGE	G.9	E-02: 0.032	H-04: 27.29	H-04: 1.12	1.11	0.063	0.07	0.358	0.575	1.04
	AIE	G.14	H-02: 0.061	H-02: 19.18	H-04: 1.12	1.11	0.092	0.098	0.103	0.358	1.03
	SEE	G.19	E-02: 0.256	E-02: 2.865	H-04: 1.10	1.09	0.258	0.259	0.26	0.118	1.03
3ph 90 %	BFO	G.5	E-02: 0.924	E-02: 1.206	H-04: 1.19	1.14	0.924	0.947	0.968	0.986	1.06
	KGE	G.10	E-02: 0.915	E-02: 0.7526	H-02: 1.16	1.14	0.919	0.919	0.943	0.965	1.09
	AIE	G.15	E-02: 0.916	H-04: 0.4596	H-04: 1.04	1.03	0.919	0.92	0.924	0.946	1.05
SvK	SEE	G.20	E-02: 0.078	E-02: 31.54	H-04: 1.03	1.03	0.046	0.042	0.04	0.063	1.03

A minimum voltage of 0.014 pu (0.38 kV) is to be found at turbine E-02 due to a three phase to ground fault in BFO, as seen in Figure 7.8

A maximum voltage of 1.52 pu (40.95 kV) is to be found at turbine H-04 due to a three phase to ground fault in BFO, as seen in Figure 7.8.

A maximum difference of 91.48 % in amplitude between two phases is found at turbine H-02, during a line to line fault at BFO.

At the platform, the low voltage side of the main transformer will experience a maximum voltage of 1.34 pu (36.1 kV) when there is a three phase to ground fault at BFO.

The minimum voltage registered at BFO due to the SvK voltage profile applied at SEE, is 0.046 pu (5.18 kV). At the turbine E-02 the minimum voltage due to this fault is 0.078 pu (2.10 kV).
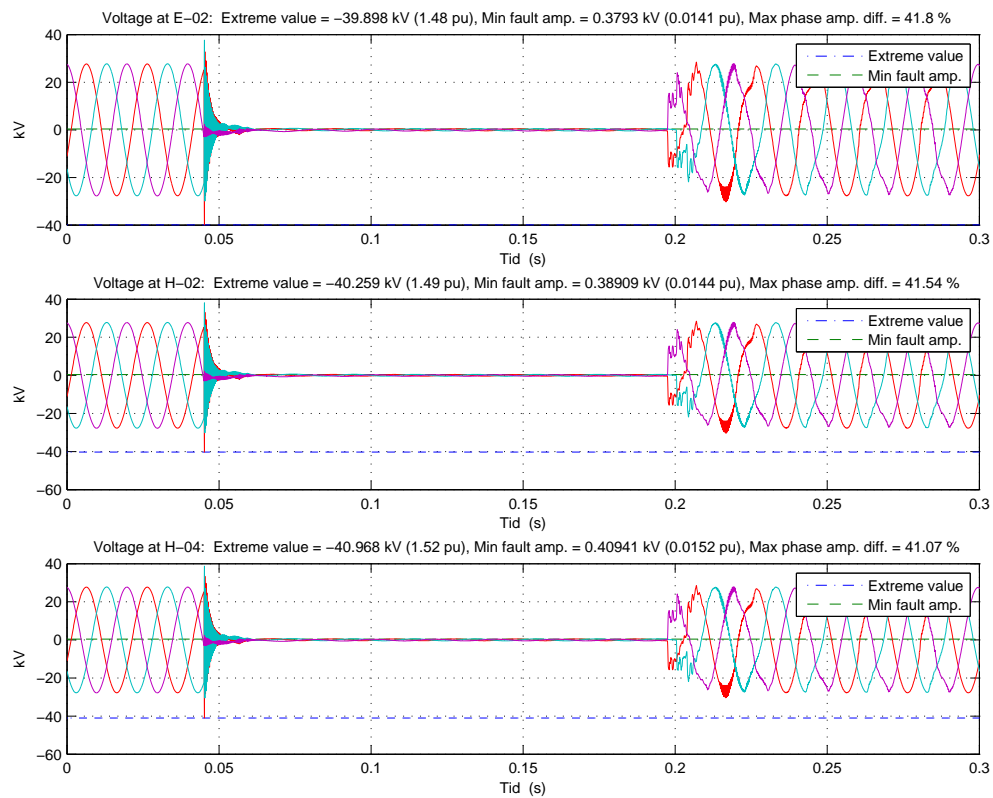
Figure 7.8 Turbine voltages due to a three phase fault in BFO when radial 1 is connected and the turbines operate at maximum.

7.5 Simulation Results

A three phase to ground fault at BFO when radial 1 is operating at full power output will cause the lowest voltage level at Lillgrund for all simulations. It will cause a minimum phase to ground voltage $|\hat{U}|_{min}$ of 0.014 pu (0.38 kV) at turbine E-02.

The maximum over voltage $|\hat{U}|_{max}$ between phase and ground that has been registered during all simulations, is 1.65 pu (44.51 kV) at turbine F-06 when the fault begins. This over voltage is due to a three phase to ground fault in KGE when all radials are connected and Lillgrund is on idle operation. The results from the four different configurations are seen in Table 7.5.

Table 7.5 Results-Voltages at the turbines

Generation Modes	Turbines	
	Maximum peak value.	Minimum peak value.
All radials, Max	F-06: 1.62 pu - 3ph at KGE	A-01: 0.101 pu - 3ph at AIE
All radials, Idle	F-06: 1.65 pu - 3ph at KGE	F-06: 0.045 pu - 3ph at BFO
Rad 1, 2, 5, Max	F-06: 1.59 pu - 3ph at KGE	A-01: 0.041 pu - 3ph at BFO
Rad 1, Max	H-04: 1.52 pu - 3ph at BFO	E-02: 0.014 pu - 3ph at BFO

The maximum over voltage due to a single line to ground fault is 1.22 pu (37.87 kV) when the fault is cleared. This is the case when the fault is applied at the BFO substation and Lillgrund operates at maximum power output with all radials connected. The maximum over voltage due to a line to line fault is 1.59 pu (42.8 kV) at the beginning of the fault. This is the case when the fault is applied at the BFO substation and Lillgrund operates at maximum power output with all radials connected.

The main transformer at the platform will experience a maximum over voltage between phase and ground when Lillgrund is on idle operation and all radials are connected. The maximum voltage $|\hat{U}|_{max}$ at the low voltage side of the transformer, is 1.56 pu (42.03 kV) due to a three phase to ground fault at KGE. The maximum voltage between phase and ground $|\hat{U}|_{max}$ at the high voltage side, is 1.17 pu (131.86 kV) due to a line to line fault at BFO. The results from the four different configurations are seen in Table 7.6.

Table 7.6 Results-Voltages at the main transformer

Generation Modes	Main transformer voltage peak	
	LV side	HV side
All radials, Max	1.55 pu - 3ph at KGE	1.14 pu - SLG ($\hat{U}$) at BFO
All radials, Idle	1.56 pu - 3ph at KGE	1.17 pu - LL at BFO
Rad 1, 2, 5, Max	1.51 pu - 3ph at KGE	1.16 pu - SLG ($\hat{U}$) at BFO
Rad 1, Max	1.34 pu - 3ph at BFO	1.15 pu - SLG ($\hat{U}$) at BFO

For all simulated configurations of connected radials, a single line to ground fault applied at crest ($\hat{U}_a$) will cause higher over voltages than those applied at zero crossing $|U_a| = 0$.

8   Conclusions

The main purpose of this thesis was to build a model of the connecting grid and to find what type of faults in the connecting grid should be dimensioning for Lillgrund. The obtained knowledge from these simulations can be used when designing future wind farms. A previous wind turbine model was to be improved and the turbines exposed to the highest over voltages and most severe voltage dips were to be identified.

The modeling of the connecting grid was well performed, judging not only from the power flow and voltage levels presented, but also from the reconstruction of the line to line fault and the response from it. The load flows in the PSCAD model were very close to the ones provided by E.ON.

The existing turbine model was improved with controllable current sources with the desired performance, as initially specified.

According to the results presented in section 7, the highest over voltage is caused by a three phase to ground fault one bus away from the PCC when all radials are connected and the turbines run in idle operation. This over voltage level of 1.65 pu is kept beneath $\sqrt{3}$ (1.72 pu) which is an over voltage level that can be expected. The most severe voltage dip was caused by a three phase to ground fault at the PCC.

As presented in section 7, the amount of radials connected inside the farm affects the transient voltage levels. One connected radial resulted in more severe voltage dips than when all radials were connected, but also in lower over voltages on both the turbines and the main transformer. More connected radials resulted in higher over voltages but less severe voltage dips.

The turbines subjected to the highest over voltages are those at the end of each radial, while the turbines at the beginning of each radial are subjected to the most severe voltage dips. These results confirm the results previously obtained by Vattenfall Power Consultant and the manufacturer.

What is also seen, is that turbines at shorter radials are exposed to lower over voltages and more severe voltage dips while longer radials result in higher over voltages but less severe voltage dips.

A lower power production results in higher over voltages and more severe voltage dips at both turbines and the main transformer.

A three-phase fault at PCC results in the most severe voltage dips, while a fault one bus away from the PCC results in the highest over voltages.

There are large differences between the over voltage levels on the two sides of the main transformer. The low voltage side will be exposed to the highest over voltages.

Single line to ground faults applied at $|\hat{U}|$ result in higher over voltages than faults applied at $|U_a| = 0$.

Another conclusion that can be drawn from this work, is that details that normally may be neglected play a very important role. Details like the fault position and fault impedance and how the tap changer position affects the zero sequence impedance.

9   Recommendations and Future Work

As it is now, the reactive power output of the turbines during the fault is completely dependent on the type of fault applied and how it affects the voltage phase. It is then also possible to study how Lillgrund can support the grid with reactive power during faults by injection of reactive power. The wind turbine model created for this thesis is simplified and should be improved in order to achieve better accuracy.

Additional grid components could be added to the model. Components such as adjacent power production facilities like Öresundsverket and the Högseröd Wind Farm. Along with the known protection settings, it would result in a better model where transients may result in instabilities and oscillations, affecting Lillgrund and its surroundings.

Detailed models of vacuum circuit breakers could be added in order to allow simulations of switchings together with faults.

The HVDC connection can be further improved with a model that more accurately behaves as a real HVDC connection does. The model does not necessarily need to be with converters, controllable current sources and logic circuits may be enough.

References

[1] J. Enquist. "Ride-through of Offshore Wind Parks." M.Sc thesis, Chalmers University of Technology, Göteborg, Sweden, 2007.

[2] C. Hermansson, J. Olsson. "Nollföljdsmodellering av transformatorer - Beräkningar av följdproblem vid ökad kablifiering på mellanspänningsnivå." M.Sc. thesis, Chalmers University of Technology, Göteborg, Sweden, 2007. (in Swedish)

[3] B. Gustavsen, J. A. Martinez, D. Durbak. "Parameter Determination for Modeling System Transients - Part II: Insulated Cables". *IEEE Transactions on Power Delivery*, vol. 20, July 2005.

[4] M. Bollen, A. Sannino. *EEK 215 Power Quality and Electromagnetic Compatibility.* (Course Compendium). Göteborg, Sweden: Chalmers University of Technology, Quarter 4 2004/2005.

[5] IEEE Std 1159-1995. "Recommended Practice for Monitoring Electric Power Quality." New York 1995.

[6] EN 50160. "Voltage characteristics of electricity supplied by public distribution systems." 1999.

[7] Svenska Kraftnät (2009). Internet: http://www.svk.se/Om-oss/Var-verksamhet/, accessed 24 Feb. 2009.

[8] Svenska Kraftnät (2005). "Affärsverket svenska kraftnäts föreskrifter och allmänna råd om driftsäkerhetsteknisk utformning av produktionsanläggningar", Internet: http://www.svk.se/Global/07_Tekniska_krav/Pdf/Föreskrifter/SvKFS2005_2.pdf, accessed 24 Feb. 2009.

[9] Å. Larsson, R. Larsson. *Anslutning av större Produktionsanläggningar till elnätet (ASP)*, Elforsk 06:79, 2006 (in Swedish)

[10] S. Arnborg, Svenska Kraftnät, "VB: Fråga angående SvKFS 2005:2" Personal E-mail (15 Dec. 2008).

[11] J. Daalder, T. A. Le. *ENM050 Power System Analysis.* (Course Compendium). Göteborg, Sweden: Chalmers University of Technolgy, September 2007.

[12] B. Stenborg. *Elkraftsystem Del 2 Analys av onormala tillstånd.* Göteborg, Sweden: Kompendiet, Göteborg 2007 (in Swedish)

[13] J. Daalder, K. Bhattacharya *Elsystem 1.* (Course Compendium). Göteborg, Sweden: Chalmers University of Technolgy, 2005.

[14] J. Duncan Glover, M. S. Sarma, T. J. Overbye. *Power System Analysis and Design.* USA: Thomson Learning 2008.

[15] "Lillgrund vindkraftpark." Internet: http://www.vattenfall.se/www/vf_se/vf_se/
518304omxva/518334vxrxv/518814vxrxe/521124omxvi/521154vxrax/
522474lillg/index.jsp, Oct. 6 2008 [Feb. 23 2009].

[16] Lillgrund location. Internet: http://www.vattenfall.se/www/vf_se/vf_se/Gemeinsame
_Inhalte/DOCUMENT/196015vatt/815691omxv/819774vxrx/879800aktu/884903lill/
P02117203.pdf, [Feb. 24 2009].

[17] M. Lindgren, D. Söderberg, A. Dahlgren. *Design av elsystem för havsbaserade vind-kraftparker*, Elforsk 08:14, 2008 (in Swedish)

[18] "Nysted Havmøllepark - The construction of Nysted Offshore Wind Farm."
Internet: http://www.dongenergy.com/NR/rdonlyres/24923A03-5705-4C3C-871B-
8DD2A4FC3AE6/0/WEB_NYSTED_UK.pdf, [Feb. 23 2009].

[19] "Horns Rev Offshore Wind Farm." Internet: http://www.hornsrev.dk/index.en.html,
[Feb. 23 2009].

[20] "Princess Amalia windpark." Internet: http://www.prinsesamaliawindpark.eu/en/
windpark.asp, [Feb. 23 2009].

[21] "Kentish Flats Offshore Wind Farm." Internet:
http://www.kentishflats.co.uk/page.dsp?area=1388, [Feb. 23 2009].

[22] "Burbo Bank." Internet: http://www.dongenergy.com/Burbo/Project/Technology/
Technology.htm, [Feb. 23 2009].

[23] "North Hoyle." Internet:
http://www.npower-renewables.com/northhoyle/statistics.asp, [Feb. 23 2009].

[24] Siemens Wind Power A/S (2008). "Grid Performance Specifications SWT-2.3-93 and
SWT-2.3-82 VS" Restricted realese. 8 Feb. 2008.

[25] T. Thiringer, Chalmers University of Technology. Conversation (Dec. 2008).

[26] M. Lindgren, Vattenfall Power Consultant Vindkraft. Conversation (Jan. 19 2009).

[27] Å. Almgren, P. Axelberg, R. Blondell, T. Cegrell, J. Hagelberg, K. A. Jacobsson, C.
Lindgren, T. Lundgren, M. Lundmark, P. Norberg, L. Wallin, R. Westöö, L. Wikman,
L. Winell, B. Åkerberg, C. Öhlén. *Elkrafthandboken Elkraftsystem 2*. Malmö, Sverige:
Elanders 2008.

[28] A. Alfredsson, K. A. Jacobsson, A. Rejminger, B. Sinner, *Elkrafthandboken Elmask-iner*. Malmö, Sverige: Elanders 2008.

[29] O. I. Elgered. *Sequence network representation of transformers in three-phase systems*. St. Louis, MO: Moloney Electric Company 1956.

[30] PSCAD help file. *The UMEC approach*. (Version 4.2.1.)

[31] "The Switch Introduces Wind Power Drive Train" Internet:
http://www.renewableenergyworld.com/rea/news/article/2009/02/the-switch-introduces-new-wind-power-drive-train?src=rss 2009-02-13 2009-02-11, [2009-02-24]

[32] J. Hansson, Vattenfall Vindkraft. "SV: Info transformatorer på Lillgrund" Personal E-mail (4 Nov. 2008).

[33] Siemens (2007). "Test certificate No.: D416 685." Dresden 4 Jan. 2007.

[34] C. A. Andersson, E.ON Elnät. "Nätdata E.ON" Personal e-mail (Oct. 16 2008).

[35] P. O. Lindström, Vattenfall Elnät. "VB: Indata till exjobb" Forwarded personal e-mail (Oct. 27 2008).

[36] C. A. Andersson, E.ON Elnät. Phone conversation (Nov. 18 2008).

[37] C. A. Andersson, E.ON Elnät. Phone conversation (Nov. 25 2008).

[38] P. Hjalmarsson, Vattenfall Power Consultant Vindkraft. Conversation (Dec. 2008).

[39] Baltic Cable. Internet: http://www.balticcable.com/, [Feb. 24 2009].

[40] D. Löfgren, Vattenfall Power Consultant Elnät. "House and Touttle.xls" Personal e-mail (Nov. 25 2008).

[41] ABB. "XLPE Underground Cable Systems User's guide rev. 3." Internet:
http://library.abb.com/global/scot/scot245.nsf/veritydisplay/1e286b0cdad18e9ec125
71cc003a3df3/$File/XLPE%20Cable%20Systems%20Users%20Guide%20rev%203.pdf
[Feb. 24 2009]

[42] Satellite photographies. Internet: http://kartor.eniro.se/, (Dec. 2008).

[43] Decision by reference group (Nov. 17 2008).

[44] D. Söderberg, Vattenfall Elnät. Conversation (Dec. 19 2008).

APPENDIX

A Appendix: Transformer configuration

Figure A.1 An example of transformer configuration parameters.

B Appendix: Equations

Equation B-1

$$C_c = 12 * 0.281 uF = 3.372 uF \tag{B-1}$$

C Appendix: Tolerance against stationary disturbances in voltage and frequency
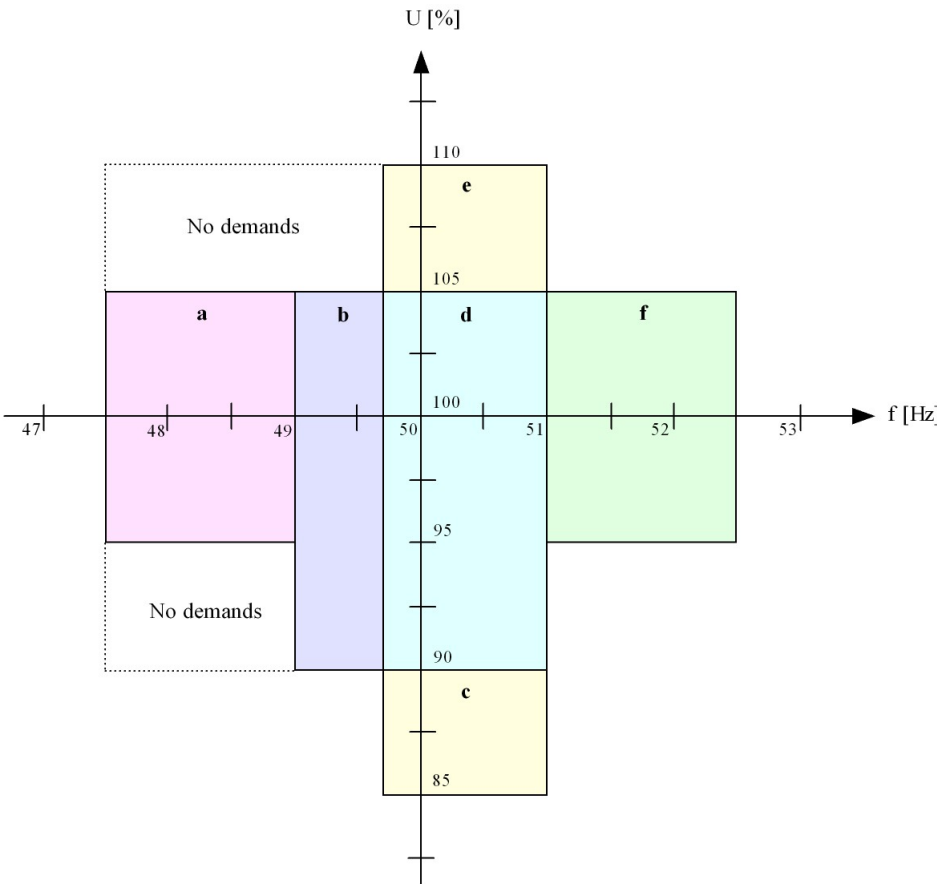

Figure C.2 Tolerance against stationary disturbances in voltage and frequency.